AN ARM-MOUNTED ACCELEROMETER AND GYRO-BASED 3D CONTROL SYSTEM

THOMAS YOUNG

A THESIS SUBMITTED TO THE FACULTY OF GRADUATE STUDIES

IN PARTIAL FULFILLMENT OF THE REQUIREMENTS FOR THE DEGREE OF

MASTER OF SCIENCE

GRADUATE PROGRAM IN COMPUTER SCIENCE AND ENGINEERING

YORK UNIVERSITY,

TORONTO, ONTARIO

JUNE 2016

ABSTRACT

This thesis examines the performance of a wearable accelerometer and gyroscope-based system for capturing arm motions in three dimensions. Two experiments conforming to ISO 9241-9 specifications for non-keyboard input devices were performed. The first experiment, modeled after the Fitts' law paradigm described in ISO 9241-9, utilized the wearable system to control a telemanipulator. The experiment compared three control modes: the wearable system, joystick control of the telemanipulator, and the user's arm. The throughputs were 5.54 bits/s, 0.74 bits/s and 0.80 bits/s, for the user arm, joystick, and wearable system, respectively. The second experiment utilized the wearable system to control a cursor in a 3D fish-tank virtual reality setup. The participants performed a three dimensional Fitts' law task with three methods for selection: button clicks, dwell, and a twist gesture. The throughput of the system ranged from 0.8 to 1.0 bits/s. Error rates were 6.82 % for click, 0.00% for dwell, and 3.59 % for the twist methods. The thesis includes detailed analyses on lag and other issues that present user interface challenges for systems that employ human-mounted sensor inputs to control a telemanipulator apparatus.

ACKNOWLEDGEMENTS

I would like to thank my family for the support and encouragement they have provided me over the years for this work. Without their dedication and steadfast devotion, this would not have been possible.

My gratitude towards my supervisor Prof Scott MacKenzie cannot be easily expressed. His support and guidance from the very beginning in letting me choose my thesis work in my area of interest, and in each step of the process from experimental design through data analysis have been invaluable.

I would also like to thank Steven Castellucci, Rob Teather and Matthew Cutone for their kind generosity and support. From discussing ideas, providing feedback, to providing hardware for my experiments I could not have done this without them.

Many thanks are also given to the Rob Allison for his support and advice, Nick Cercone who unfortunately passed away before the completion of my thesis but who had given me wonderful encouragement and support from the beginning, and last but not least Ouma Jaipaul Gill for helping me through every step of graduate school.

TABLE OF CONTENTS

ABSTRACT…………………………………………………………..ii

ACKNOWLEDGEMENTS……………………………..……………..iii

TABLE OF CONTENTS…………………………………………………..iv

LIST OF TABLES…………………………………………………vii

LIST OF FIGURES..viii

CHAPTER 1 - INTRODUCTION...1

1.1 Introduction.. 1

1.1.1 Positioning and Orienting Objects in 3D Space.. 2

1.1.2 Joysticks.. 4

1.1.3 Motion Capture of Human Movements.. 6

1.2 Thesis Contribution.. 10

CHAPTER 2 - BACKGROUND...12

2.1 Related Work.. 12

2.1.1 Joysticks.. 12

2.1.2 Fitts' Law.. 12

2.1.3 Game Controllers and Spatially Convenient Devices 15

2.1.4 Teleoperated Systems 16

2.1.5 3D Pointing 19

2.1.6 Jitter, Latency, and Lag.. 24

CHAPTER 3 - EXPERIMENT 1...26

3.1 Methodology 26
3.1.1 Participants 31
3.1.2 Apparatus 31
3.1.3 Task and Target Parameters 32
3.1.4 Procedure 33
3.1.5 Design 34
3.2 Results 34
3.2 Discussion 40
CHAPTER 4 - EXPERIMENT 2 46
4.1 Methodology 46
4.1.1 Participants 49
4.1.2 Apparatus 50
4.1.3 Target Parameters 51
4.1.4 Procedure 52
4.1.5 Design 52
4.2 Results 53
4.3 Discussion 59
CHAPTER 5 - DISCUSSION 66
5.1 The Wearable System 66
5.2 Latency Issues 66
5.3 Sensor Issues 67
5.4 System Design Considerations 68

CHAPTER 6 - CONCLUSIONS AND FUTURE WORK............................71

REFERENCES...73

LIST OF TABLES

Table 1: Experiment 1 independent variables and levels. 34

Table 2: Comfort, effort, and ease use ratings for experiment 1. 37

Table 3: Grand means for joystick, user arm, and wearable control modes. 40

Table 4: Throughputs for user arm and telemanipulator system comparison 41

Table 5: Experiment 2 independent variables and levels. 53

Table 6: Comfort, effort and preference ratings for experiment 2. 56

Table 7: Grand means for click, dwell, and twist selection methods. 59

LIST OF FIGURES

Figure 1: Spatial coordinate systems. 3

Figure 2: Orientation representations - Euler Angles (left), pitch, roll, azimuth (right)........ 3

Figure 3: An operator using a joystick to control the Canadarm from the Missions Operations Station of the Canadian Space Agency... 4

Figure 4: Plus Tech OY *Forestry Excavator* (left), Controls (right). 5

Figure 5: Logitech *Extreme 3D Pro* (left), Logitech *F310 Gaming Gamepad* (right). 6

Figure 6: GE *Handyman*. 7

Figure 7: NaturalPoint *OptiTrack* camera setup.. 8

Figure 8: A user study participant with the wearable control device. 9

Figure 9: Two dimensional Fitts' law task. 14

Figure 10: Vergence accommodation conflict.. 20

Figure 11: Target shapes - 3D sketches and corresponding 2D views. 23

Figure 12: Fitts' experimental apparatus. 27

Figure 13: Test apparatus for use with the Lynxmotion *AL5D* robotic arm. 27

Figure 14: User arm control mode. 28

Figure 15: Joystick control control mode. 28

Figure 16: Wearable control mode. 29

Figure 17: Lynxmotion AL5D. 30

Figure 18: Throughput by control mode. Error bars show ±1 *SE*. 35

Figure 19: Movement time by control mode. Error bars show ±1 *SE*. 36

Figure 20: Error rate by control mode. Error bars show ±1 *SE*... 36

Figure 21: Comfort level. Higher scores are better. Error bars shows ±1 *SE*. 38

Figure 22: Ease of use. Higher scores are better. Error bars shows ±1 *SE*. 38

Figure 23: Effort level. Lower scores are better. Error bars show ±1 *SE*. 39

Figure 24: Ergonomic button click controller. 47

Figure 25: Click method.. 48

Figure 26: Twist method. 49

Figure 27: 3D cursors skitter (left) jack (right). 50

Figure 28: Fitts' 3D task. 51

Figure 29: Movement time by selection method. Error bars show ±1 *SE*. 54

Figure 30: Error rate by selection method. Error bars show ±1 *SE*.................................... 54

Figure 31: Calculating the effective index of difficulty (ID_e). 55

Figure 32: Throughput by selection method. Error bars show ±1 *SE*............................... 56

Figure 33: Comfort level by selection method. Higher scores are better. Error bars show ±1 *SE*. 57

Figure 34: Effort level by selection method. Higher scores are better. Error bars show ±1. *SE*. 58

Figure 35: Preference by selection method. Higher scores are better. Error bars show ±1 *SE*. 58

Figure 36: Correct orientation for twist method. 63

Figure 37: Incorrect orientation for twist method.. 64

CHAPTER 1 - INTRODUCTION

1.1 Introduction

Recent innovations in sensor technology have facilitated the creation of a class of spatially convenient devices characterized by three-dimensional input data, useful sensors and interface options, low cost, and easy configuration. We have designed such a device for interacting with objects in the real and virtual three-dimensional worlds. Real-world applications include industrial control, surgery, construction, and bomb disposal. Virtual applications are found in CAD/CAM, 3D gaming, and virtual and augmented reality. In this research, we focus on target selection via telemanipulation (the remote manipulation of objects) in the real world, and target selection in stereoscopic VR (virtual reality). Telemanipulation is a standard function in many modern robots. This capability is needed for handling hazardous materials such as nuclear waste and explosives, or operating in hostile environments, underwater, or in low-earth orbit.

Telemanipulation robots may also function at scales significantly different from humans such as the nano-manipulation of single atoms or molecules. Historically, controllers for telemanipulation consist of joysticks, keyboards, and other non-intuitive systems. Since these systems often require significant training time and may be difficult, awkward, or cumbersome, issues of operator performance arise.

Our wearable inertial three-dimensional control device captures the arm motions of a human operator to position a robotic arm. It is referred to as an *inertial controller* because particular accelerations and rotations are measured and employed. Performance is compared with the de facto joystick standard for telemanipulation. In three-dimensional computing however, no such standard device exists. Traditional devices for three-dimensional tracking include the Ascension *Flock of Birds*[1], the Polhemus *Patriot*[2], and the NaturalPoint *OptiTrack*[3]. These devices are relatively expensive and some setups, such as systems using the *OptiTrack*, are not portable and require a fixed installation in a specific frame of reference.

Three-dimensional input devices for gaming such as the Nintendo *Wiimote* and the Sony *Playstation Move* are economical, but require cameras and optical sensors to determine their position in space, much like the *OptiTrack*. Our device is portable, self-contained, easy to set up, and an order of magnitude cheaper than the traditional tracking devices. We evaluate the performance of our device and compare it to previous results with the NaturalPoint *OptiTrack*.

1.1.1 Positioning and Orienting Objects in 3D Space

Telemanipulation robots work in three-dimensional (3D) space. To fully describe the position and orientation of an object, three spatial and three rotational parameters are required. These descriptions may be represented in various forms. Positions may be given in Cartesian, cylindrical, or spherical coordinates (Figure 1). Orientations may be specified

---

[1] http://www.5dt.com/products/pfob.html

[2] http://polhemus.com/motion-tracking/all-trackers/patriot/

[3] http://www.optitrack.com/

with pitch, roll, and azimuth, or Euler Angles (Figure 2). Thus, a telemanipulation controller must have at least six degrees of freedom to completely position and orient an object.

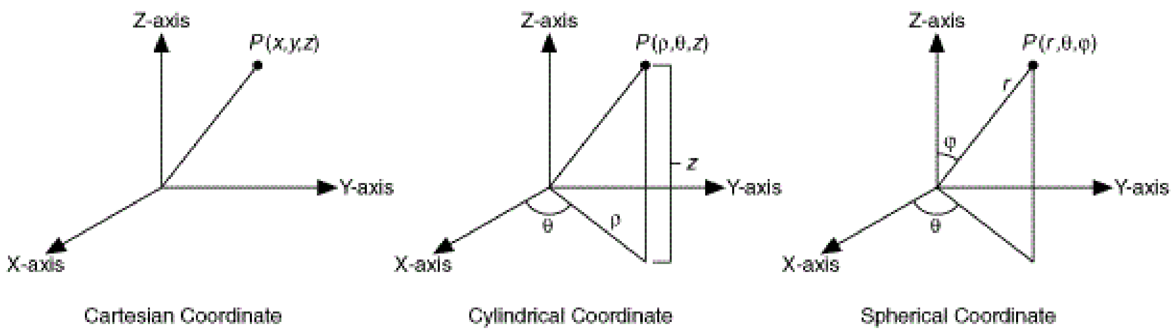

Figure 1: Spatial coordinate systems.[4]

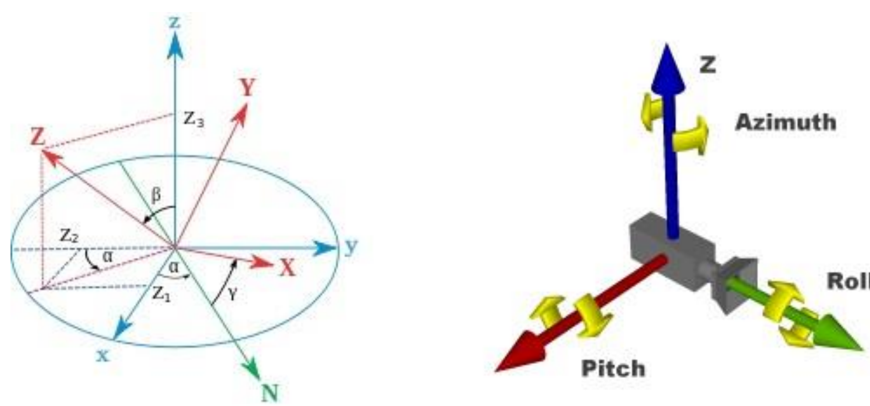

Figure 2: Orientation representations - Euler Angles[5] (left), pitch, roll, azimuth[6] (right).

---

[4] http://zone.ni.com/reference/en-XX/help/371361J-01/gmath/3d_coordinate_conversion/

[5] https://en.wikipedia.org/wiki/Euler_angles

[6] http://www.spaceyes3d.com/plugin/doc/group___camera.html

1.1.2 Joysticks

A standard method of positioning a telemanipulator utilizes joystick controls. Examples include the Canadarm at the Missions Operations Station of the Canadian Space Agency (Figure 3), the Plus Tech OY forestry excavator (Figure 4), forklifts, cranes, and other varieties of equipment in industries such as oil and gas.

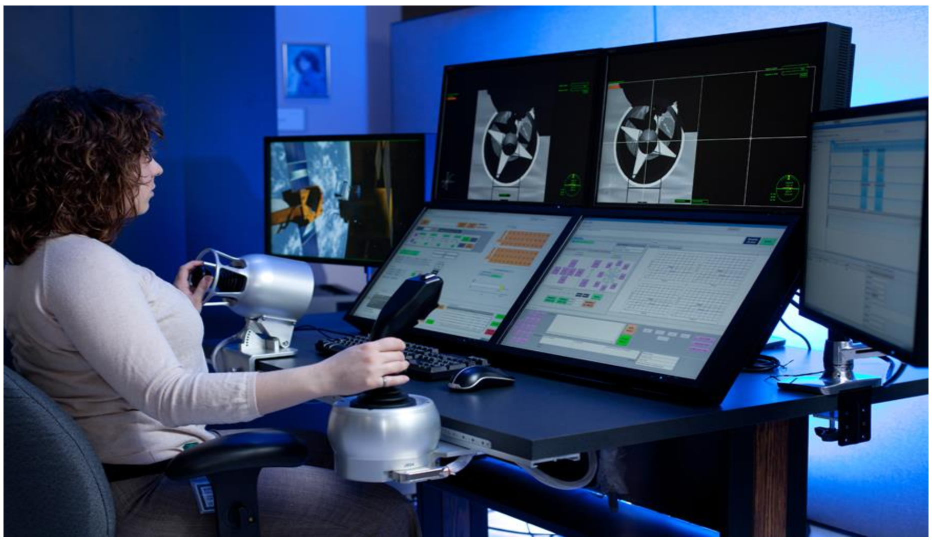

Figure 3: An operator using a joystick to control the Canadarm from the Missions Operations Station of the Canadian Space Agency.[7]

[7] http://www.asc-csa.gc.ca/eng/canadarm/ngc.asp

Figure 4: Plus Tech OY *Forestry Excavator* (left), Controls (right).[8]

A joystick in its basic form has two degrees of freedom along two perpendicular axes. However, as more degrees of freedom are required, the controllers grow more complicated and less intuitive. The Canadarm, for example, has six degrees of freedom consisting of two shoulder joints, an elbow joint, and three wrist joints (Kauderer, 2013). It requires two separate controllers, one for rotational and another for translational movements. Designed for flight simulators, the Logitech *Extreme 3D Pro* (Figure 5) has forward, backward, right, left, and twist controls, and an eight-way hat switch (a mini joystick on top of the handle). The Logitech *F310 Gaming Gamepad* utilizes two joysticks, seven buttons, a directional pad, and a right and left trigger (Figure 5). Keeping track of so many control options is mentally demanding and requires significant training.

[8] http://www.deere.com

There are two types of joysticks. Isometric joysticks have a stationary handle that senses the force applied in a specific direction or angle. Displacement (aka isotonic) joysticks measure the position of a moveable handle. Additionally, there are two forms of joystick control: zero order (position control) and first order (rate control). A joystick moving a cursor on a computer screen with zero order control determines its position, and with first order control determines its movement speed.

Figure 5: Logitech *Extreme 3D Pro* (left), Logitech *F310 Gaming Gamepad* (right).[9]

1.1.3 Motion Capture of Human Movements

The most intuitive method of pointing, reaching, or grasping is with one's own arm – a skill learned in infancy. There are many ways to capture the motion of a human arm. The GE *Handyman* (Figure 6), a two-armed robot developed in 1958 for work on nuclear-powered aircraft, is controlled by sensors in an exoskeleton worn by the operator.

[9] http://www.logitech.com/

Hollywood studios sometimes use camera systems to capture human kinematics for control of proxy actors or avatars. The Microsoft *Kinect* game controller uses an infrared projector and camera to capture motion in three dimensions, and can be been used to control a robot (Koo et al., 2013). The Sony *Playstation Move* utilizes a camera in addition to inertial and rate sensors to determine position as well as orientation. The Nintendo *Wii Mote* similarly utilizes accelerometers in combination with optical sensors.

Figure 6: GE *Handyman.*[10]

The NaturalPoint *OptiTrack* motion capture system requires a fixed installation of cameras (Figure 7) with fiduciary markers placed on the subject.

---

[10] http://www.ge.com

Figure 7: NaturalPoint *OptiTrack* camera setup.[11]

In our research, a low-cost self-contained control device in a wearable system was designed and constructed for the teleoperation of a robotic arm (Figure 8) in a master-slave manipulator configuration. The system is based on six-degree-of-freedom gyro and accelerometer sensors. Each sensor reads its orientation and any acceleration experienced in three-dimensional space. The sensors are worn on the forearm and upper arm. Rotations in three dimensions about the shoulder and elbow are registered. The system is self-contained and unobtrusive, and, hopefully, will be easy to use. The operator's arm movements are sensed and used to position the end effector of a robotic arm.

[11] http://www.optitrack.com

Figure 8: A user study participant with the wearable control device.[12]

[12] Young, T. (Photographer). 2012.

1.2 Thesis Contribution

Low-cost single-chip solutions incorporating accelerometer and gyro sensors are relatively new. While they are ubiquitous in modern mobile phones and game controllers, there has been relatively little exploration of their utility as computer interface devices. This thesis explores the design space of an accelerometer/gyro-based wearable system through two experiments. In the first experiment, the performance of the wearable system was compared to that of a traditional joystick in the control of a telemanipulator performing a Fitts' law reciprocal tapping task. An addition point of comparison involved the participant performing the same task by hand. Not surprisingly, direct performance by hand through the user's own arm achieved the highest throughput at 5.54 bits/s. The two wearable methods yielded significantly lower throughput, just under 1.0 bits/s.

The second experiment utilized the wearable system to control a cursor in a three-dimensional fish-tank virtual reality setup. The participants performed a three dimensional reciprocal tapping task with three selection methods: button clicks with an ergonomic controller, dwell, and a novel twist gesture. The overall throughput of the system ranged from 0.80 to 0.95 bits/s. Error rates were 6.82 % for click, 0.00% for dwell, and 3.59 % for the twist methods.

1.3 Thesis Organization

The rest of the thesis is organized as follows:

Chapter 2. Related work is presented including Fitts' Law, with extensions to higher dimensions, joysticks and game controllers, teleoperation, spatially convenient devices, 3D pointing, jitter, latency and lag.

Chapter 3 focuses on Experiment 1, a Fitts' law reciprocal tapping task in one dimension with both our wearable control mode and joystick control of a telemanipulator. These are compared to a replication of Fitts' original experiment where users selected targets by hand with a stylus. The experiment used the one-dimensional protocol described in ISO 9241-9.

Chapter 4 focuses on Experiment 2, a three-dimensional fish-tank virtual reality reciprocal tapping task with three different selection methods. The virtual environment was created through stereoscopic glasses and a three dimensional monitor.

Chapter 5 discusses both studies including issues with the wearable system, latency, and system issues.

Chapter 6 presents conclusions and future work for evaluation and discussion on improvements to the system design.

CHAPTER 2 - BACKGROUND

2.1 Related Work

2.1.1 Joysticks

A large body of work exists examining joysticks and their performance. The studies often involve selection tasks on computer screens (e.g., Card et al., 1978; Douglas, 1999; Epps, 1986). Some studies evaluated isometric joysticks while others examined isotonic joysticks. Joystick performance was also evaluated in the context of video game controllers (Natapov et al., 2009).

A study of joystick rate control versus position control compared the two modes using the Argonne National Laboratory *ANL E2* manipulator in simulated pick-and-place tasks (Kim et al., 1987). Position control yielded superior results when the workplace was small relative to the operator. Position and rate control methods were also evaluated for 3D pointing tasks with isotonic and isometric controllers (Schmitt et al., 2012). It was determined that isotonic control was more efficient than isometric control. Control modes in heavy equipment teleoperation were summarized, listing the advantages and disadvantages of each (Lapointe et al., 2001).

2.1.2 Fitts' Law

A standard methodology in the evaluation of non-keyboard input devices is contained in ISO 9241-9 to measure performance and comfort (ISO 2000; Soukoreff and MacKenzie, 2004). The primary dependent variable of interest is throughput (MacKenzie, 1992:

MacKenzie, 2015) derived from Fitts' Index of Performance (Fitts, 1954). Throughput (*TP*, in bits per second) is computed as the ratio of the index of difficulty (*ID*, in bits) to the movement time (*MT*, in seconds) averaged over a sequence of trials (Eq. 1):

$$TP = \frac{ID_{average}}{MT_{average}} \qquad (1)$$

ID is calculated as the logarithmic ratio of the movement distance *A* over the target width *W* plus a constant factor in what is known as the Shannon formulation (Eq. 2):

$$ID = \log_2\left(\frac{A}{W} + 1\right) \qquad (2)$$

Rather than the presented *IDs* (Eq. 2), the ISO standard uses effective *IDs* (Eq. 3) to accommodate the accuracy or variability in targeted selections observed in the movements of test subjects (MacKenzie, 1992):

$$ID_e = \log_2\left(\frac{A_e}{4.1333 \times SD_x} + 1\right) \qquad (3)$$

The A_e term is the effective distance a test subject actually moved between targets. SD_x is the standard deviation of x (the coordinates of target hits) over a sequence of trials. However, these effective terms can only be calculated when the coordinates of the target hits can be determined. In Fitts' original experiment, this was not possible since only a hit or miss, but not position, was registered. Alternately, ID_e and A_e can be determined using the discrete error method as described by MacKenzie (1992).

Other formulations for *ID* exist, but may yield problematic results. For example, in some formulations a negative *ID* sometimes occurs. This is avoided using the Shannon formulation.

Fitts' Law was extended to two dimensions (MacKenzie and Buxton, 1992; Murata, 1999) and three dimensions (Murata and Iwase, 2001). In the three-dimensional formulation, a direction parameter was included giving a better fit to the conventional model. Fitts' law has also been extended to three-dimensional pointing tasks (Cha and Myung, 2013).

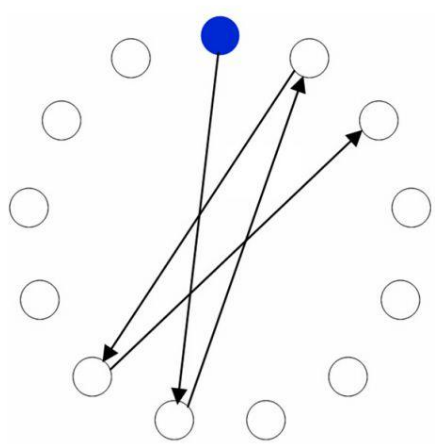

Figure 9: Two dimensional Fitts' law task.[13]

[13] Teather 2011

A factor that may affect theoretical performance between control modes is discrepancies in the source of movements and movement amplitudes. Joysticks are controlled by finger movements, whereas our wearable system is controlled by arm movements. One study has demonstrated that smaller movements yield higher throughputs on the order of 38 bits/sec for finger motion as opposed to 10 bits/sec for arm motions (Langolf et al., 1976). However, these results were re-examined in view of a contemporary understanding of Fitts' throughput and new figures were obtained: 3.0 bits/sec for the unsupported index finger, and 4.1 bits/sec for the wrist and forearm (Balakrishnan and MacKenzie, 1997).

In the positioning of joints and limbs, it was determined that humans are able to discriminate angular position more accurately in proximal versus distal joints[14] (Biggs and Srinivasan, 2002).

2.1.3 Game Controllers and Spatially Convenient Devices

A class of *spatially-convenient* devices characterized by three-dimensional input data, low cost, useful sensor and interface options, and easy configuration was conceptualized (Wingrave et al., 2010). These devices are ubiquitous through the gaming world and modern mobile phones. Examples include the Nintendo *Wii Mote* and the PlayStation *Eye*. The *Wii Mote* uses inertial sensors combined with an optical sensor to generate acceleration data in three dimensions without a particular frame of reference. The PlayStation *Eye* is a

[14] Proximal meaning closer to the body; distal meaning further.

camera that uses motion detection to capture human activity for gaming purposes. Both devices are inexpensive and easily configurable.

Many studies have focused on aspects of inertial sensors, such as game-controller performance (McArthur et al., 2009), novel applications of inertial game controllers (Gallo et al., 2008), inertial algorithms (Van Laerhoven et al., 2003), sensor networks for motion capture (Farella et al., 2007), sensor networks as game controller input (Crampton et al., 2007), and devices for disabilities (Music et al., 2009).

2.1.4 Teleoperated Systems

The performance of teleoperated systems, including surgical robots, may have different performance measures. Many studies use time to completion for specific tasks such as picking and placing objects. Measures of error rate and accuracy are also used as performance metrics. However, these measures are not useful for direct comparison between studies because the scales of tasks are not standardized across platforms. The ISO 9241-9 standard attempts to rectify this using throughput as a performance metric. Throughput is normalized for accuracy and is relatively independent of the scale of tasks employed (Soukoreff and MacKenzie, 2004). Thus, Throughput, if calculated as per ISO 9241-9, is comparable across studies. One study defined three new measures, manipulator joint effort, manipulator dexterity, and end effector motion effort (McLean et al., 1994).

Experimental results in robot-assisted surgery studies have verified predictions of Fitts' law. One study used the *da Vinci Surgical System* to measure the speed-accuracy trade-off where a significant linear correlation between *MT* and *ID* was demonstrated (Chien et al., 2010). Another study, using the Zeus surgical robot, verified the *MT* versus *ID* linear correlation in timed movement tasks (Ellis et al., 2004). The effect of control-display gain was also examined in this study. It was demonstrated that as target sizes became smaller, *MT* increases regardless of motion scaling settings. Unfortunately, effective target width was not used in their calculations hindering generalization of the results to Fitts' law.

Human performance issues in user interface design for teleoperated robots were examined in a comprehensive review of more than 150 papers (Chen et al., 2007). Issues such as lag, frame rate, video bandwidth, lack of proprioception, etc. were examined.

Teleoperator performance was evaluated by varying end-effector velocity and input frequency (Draper and Handel, 1989). End-effector velocities were either operator-paced or machine-paced, where the former is limited by human motion and the latter by the manipulator system (Goertz, 1964). Machine pacing may cause a lag between human action and manipulator response, thus impacting performance. Critical limits were found for input frequency and velocity limits which determine the pacing of the system.

One research group measured teleoperator performance by a Fitts' tapping task utilizing the ASEA *IRB-6* 5DOF robot manipulator with the NDI *Optotrack* camera based system via direct viewing of the work space (Mihelj et al., 1998). The same tapping task was performed by the test participants by the user's arm. It was found that the throughput of the teleoperated system was roughly 2 bits/s while the human throughput was 14 bits/s. A similar experiment (Draper et al., 1990) was performed with the Oak Ridge National Laboratory's *ASM* (Advanced Servomanipulator). They measured a throughput of 2.88 bits/s with the teleoperator and a throughput of 16.98 bits/s by the user's arm. The ASM control system utilized a pair of master arms replicating the remote slave manipulator arms, three 19 inch monitors with multiple camera views, and a control console. A previous study at the same lab yielded a throughput of 1.67 bits/s with the ASM and 11.27 bits/s by user arm (Draper and Handel, 1989). A study of control strategies in laparoscopic performance evaluated by a Fitts' task supported the results obtained by Draper et al. (Gonzalez et al., 2007).

The calculation of throughput in the preceding studies did not follow the practice described in ISO 9241-9; thus, the values in absolute terms are suspect and difficult to compare between studies. See MacKenzie (2015) for related discussion. While experiments not conforming to the ISO standard may have internal validity, the absence of external validity limits their usefulness for comparisons to other studies.

A study with an accelerometer/gyro system worn in a jacket was undertaken with a bomb disposal robot (Bruggemann et al., 2013). Results were mixed. Untrained operators learned to use the wearable system faster than a joystick; however, trained operators were able to use the joystick better. Tasks involving all the degrees of freedom of the manipulator were performed faster using the wearable system. It was surmised that with the joystick, operators could rest and plan between movements; however, the wearable system required the operator's arm to be properly positioned at all times, and this caused fatigue.

2.1.5 3D Pointing

A large body of work exists for object selection techniques in virtual 3D environments (Argelaguet and Andujar, 2013; Jankowski and Hachet, 2013; Hand, 1997). Most of these studies involve rays and virtual hand metaphors. One study of the classification of selection techniques proposed decomposing tasks into subtasks (Bowman et al., 1999).

The notion of input device footprint – the length of the total path an input device traveled to complete a trial – was examined in a study of 3D selection techniques for volumetric displays (Grossman and Balakrishnan, 2006). They proposed a tool called *depth ray* that reduces movement time, error rate, and input device footprint for 3D interaction.

Aimed movements in the real world were compared with movements in virtual reality (Liu et al., 2009). It was observed that there were significant temporal differences in both the ballistic and control phases. Movements in virtual reality are less efficient and on average twice as long compared to real world movements. The correction phase in virtual reality was even longer, taking an average of six times longer than real world corrections. Improvements in the correction phase in virtual reality are more efficient, but that was attributed to less of a need to correct movements in the real world.

Tactile feedback in the form of electrical muscle stimulation (EMS) and vibration were examined in the context of 3D virtual hand pointing. A Fitts' task in three dimensions demonstrated that both EMS and vibration aided in visual feedback (Pfeiffer and Stuerzlinger, 2015).

The effects of vergence - accommodation conflicts (Figure 10) were examined and determined to hinder visual performance and cause visual fatigue (Hoffman et al., 2008).

Note: The vergence-accommodation conflict occurs when the eyes rotate to focus at a specific point in space, but the individual eyes focus on a different point. In Figure 10a, both the rotation of the eyes and the focus point of each eye match the same point in physical space, however in Figure 10b, the focus point of eye rotation, and the focus point(s) of each eye are different. This is a problem inherent in stereo displays.

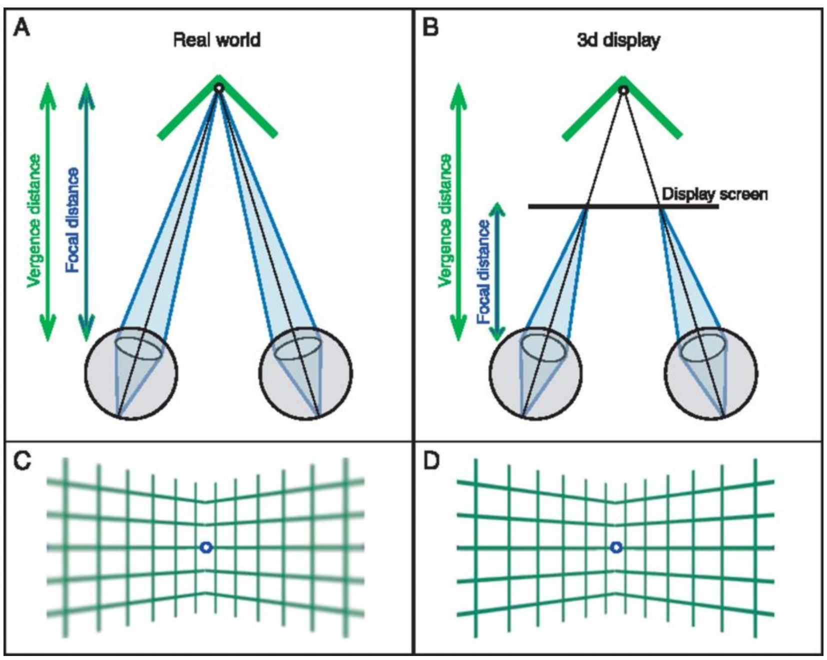

Figure 10: Vergence accommodation conflict.[15]

[15] Hoffman et al, 2008.

Design issues in air pointing interfaces were examined in a study of spatial target acquisition (Cockburn et al., 2011). It was observed that large movements on a two-dimensional plane were both rapid and accurate. Ray-casting was rapid but inaccurate while movements in three-dimensional volumes were expressive (albeit slow), inaccurate, and demanding.

Pointing at 3D targets was also studied in different contexts using a CAVE (Teather and Stuerzlinger, 2010), fish tank VR with stereo and head tracking (Teather and Stuerzlinger, 2011), and one-eyed versus stereo cursors (Teather and Stuerzlinger, 2013). In the CAVE experiment, it was determined that targets presented closer to the physical display surface were easier to hit than those displayed farther off. The results of the stereo and head tracking study supported the validity of the conventional formulation of Fitts' law in two dimensions. Motions in three dimensions however were not so well modeled, as demonstrated in previous studies. The study of one-eyed versus stereo cursors demonstrated that one-eyed cursors improve performance only when targets are presented on the screen plane and that constant target depth does not improve throughput. It was also observed that Fitts' law target parameters varying in depth yielded constant throughput in the absence of stereo cue conflicts.

The effects of stereo and head coupling in fish tank VR were examined by Ware et al. (1993) where it was determined, in the perception of depth, that head coupling was more important than stereo alone. This result was supported in a more recent similar study

(Wright et al., 2012). Participants preferred head coupling combined with stereo display for experiencing depth.

Visual aids in 3D selection tasks were also studied (Teather and Stuerzlinger, 2014). Support cylinders and texturing did not significantly affect performance; but highlighting of targets helped increase movement speed while decreasing error rate. Highlighting also helped selection in both the task axis and in the orthogonal direction.

Three dimensional target shapes and volumes were examined in the context of their visual appearance to a user performing a pointing motion (Stuerzlinger 2013). The relative advantages and disadvantages of shapes such as discs, spheres, hemi-spheres, cylinders, oriented cylinders, and oriented truncated cones were examined. Difficulties arise in displaying a three dimensional shape on a computer screen which is essentially a two dimensional surface. Factors such as viewing angle and visual profile may become problematic. While certain shapes may be advantageous in their presentation to viewers, their actual three-dimensional volume may be inaccurate thus affecting measures such as the calculation of effective target widths.

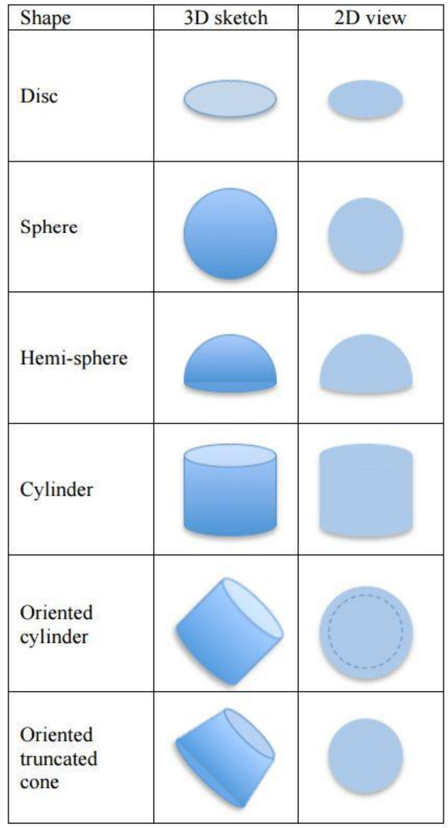

Figure 11: Target shapes - 3D sketches and corresponding 2D views.[16]

The effect of visual and motor co-location in fish-tank virtual reality was evaluated with a 3D object movement task (Teather et al., 2009). No significant differences were found between co-located and disjoint conditions, however object movements in a specific direction into the scene (depth) were faster with the co-located method.

One study of distal pointing determined that movement time was best described as a function of angular amplitude and the angular target size (Kopper et al., 2010). In contrast

[16] Sturzlinger, 2013

to Fitts' law, they demonstrated that angular target size had a significantly larger effect on movement time than angular amplitude. Additionally, the growth in difficulty for the tasks was not linear, but quadratic.

3D goal directed movements were examined in detail by dividing the movements into more distinct meaningful phases (Nieuwenhuizen et al., 2009). The effects of practice were examined in individual phases. Analysis of the individual phases of movement yielded more meaningful conclusions than analysis of overall movement. It was observed that users could benefit more from assistance in the correction phase than assistance in the ballistic phase.

2.1.6 Jitter, Latency, and Lag

The effect of lag on human performance was investigated by MacKenzie and Ware (1993). It was observed that at the highest lag tested (225 ms) movement times and error rates increased by 64% and 214% respectively while throughput decreased by 46.5%. A mathematical model was proposed with lag as a multiplicative factor in Fitts' Index of Difficulty. Lag and frame rate in VR (virtual reality) displays were also studied (Ware and Balakrishnan, 1994). Results confirmed the multiplicative factor in Fitts' Index of Difficulty. It was observed that low frame rates degrade performance and that error rates and movement times increase in depth movements as opposed to movements in planes parallel to the screen plane.

Latency and spatial jitter on object movement were examined in a study using the NaturalPoint *OptiTrack* compared to a baseline optical mouse (Teather et al., 2009). It was observed that the end-to-end latency of the mouse-based system was approximately 35 ms, while the OptiTrack was roughly 70 ms. Latency had a much stronger effect on human performance than low amounts of spatial jitter. Large spikes in jitter significantly impact 3D performance.

Human performance, as demonstrated by MacKenzie and Ware (1993), is significantly impacted by latency. A device was designed specifically to measure the latency of touch screen devices (Deber et al., 2016). This device measures the full end-to-end latency of a touch screen device as experienced by a user.

CHAPTER 3 - EXPERIMENT 1

3.1 Methodology

The performance of the wearable system was evaluated with a Fitts' Law reciprocal tapping task. The experimental apparatus was modeled after Fitts' original study (Figure 12). In the modified apparatus (Figure 13), pairs of target plates of varying sizes were placed on a surface separated by various distances. The entire surface detected errors without using error bars, as in Fitts' original study.

Alternating left and right stimulus lights indicated the desired target for selection. The stimulus lights were positioned near the top of the target plates. The test subject moved an instrument to touch the targets using one of three control modes: (i) using their own arm (Figure 14), (ii) using the robotic arm with joystick control (Figure 15), and (iii) using the robotic arm with our wearable control system (Figure 16).

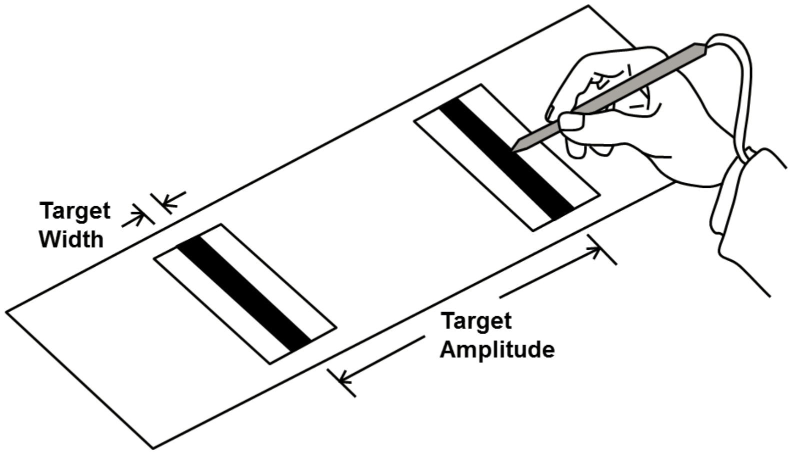

Figure 12: Fitts' experimental apparatus.[17]

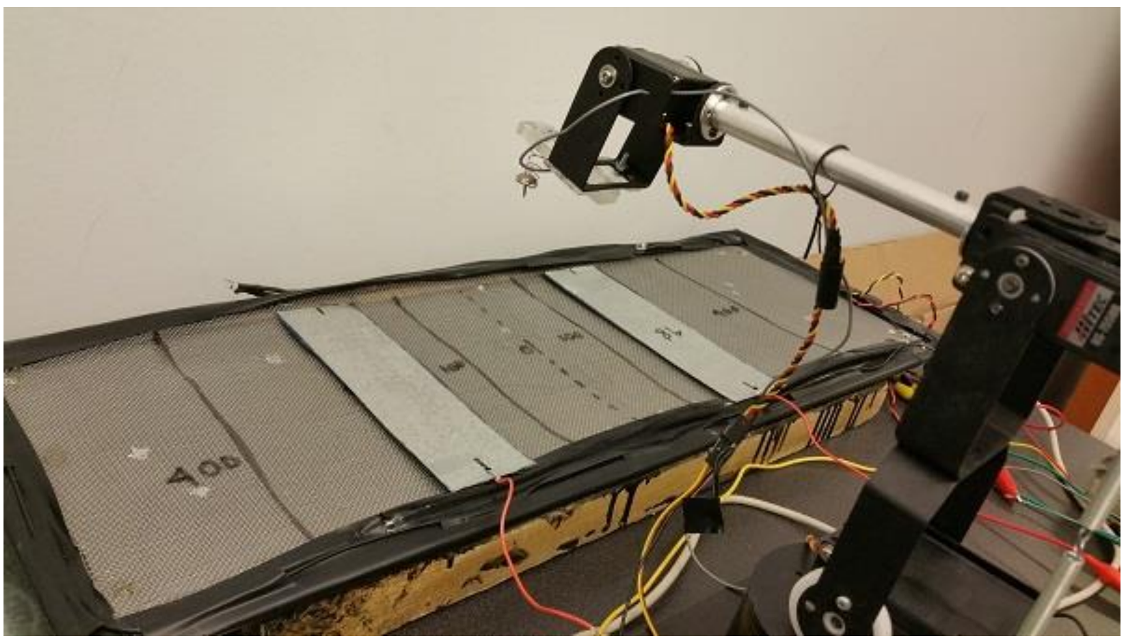

Figure 13: Test apparatus for use with the Lynxmotion *AL5D* robotic arm.[18]

[17] Fitts 1954.

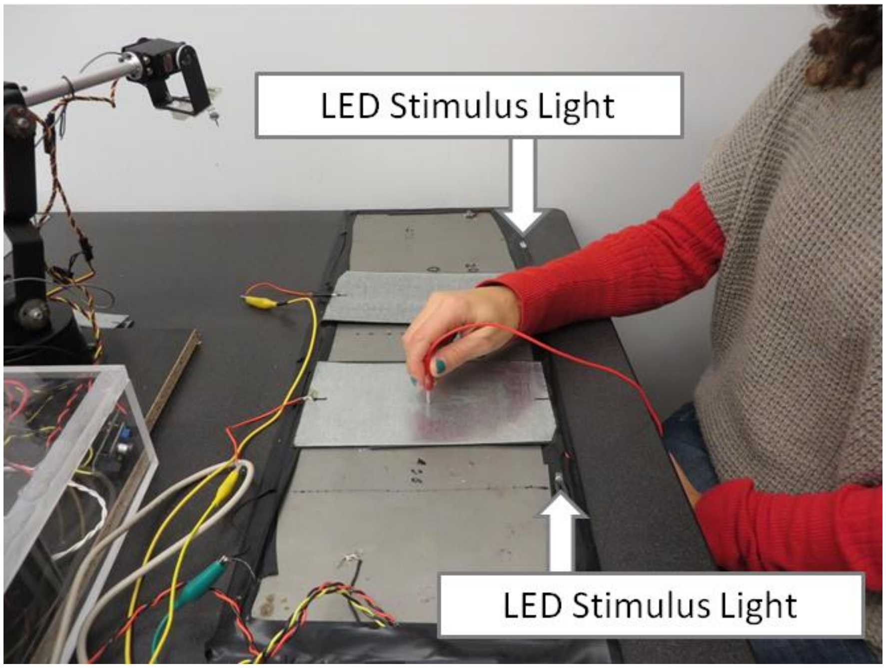

Figure 14: User arm control mode.[19]

Figure 15: Joystick control control mode.

[18] Young, T. (Photographer). 2015.

[19] Young, T. (Photographer). 2015.

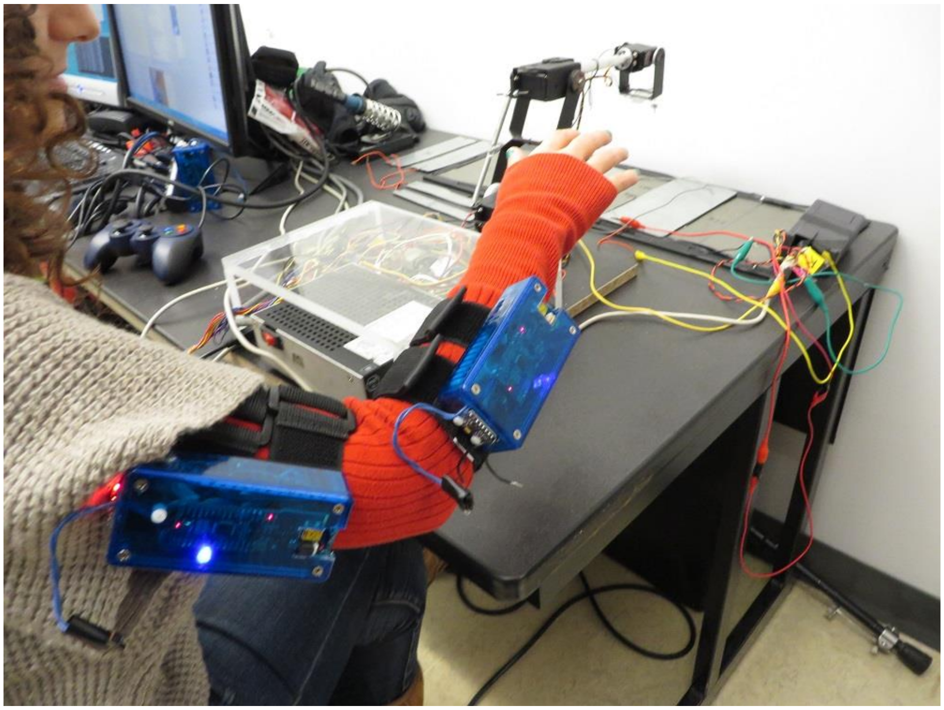

Figure 16: Wearable control mode.

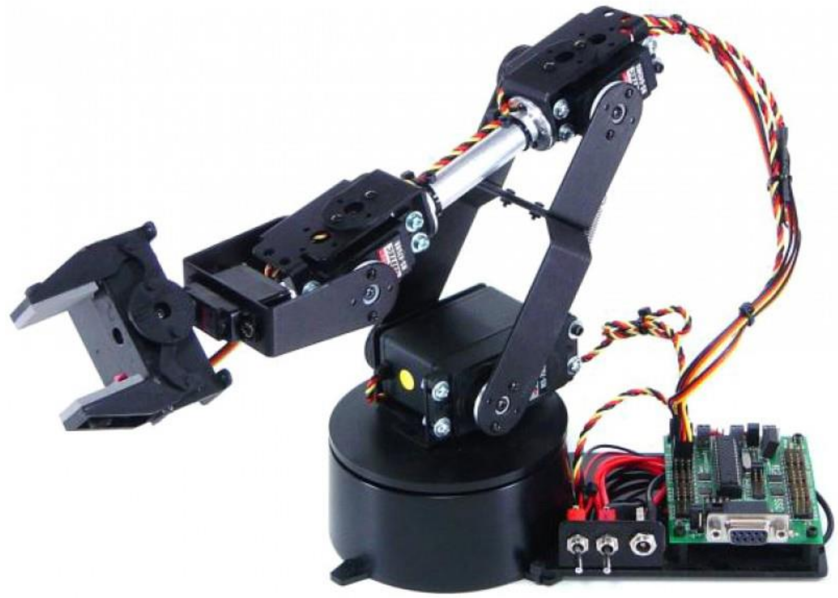

Figure 17: Lynxmotion AL5D.[20]

The robotic arm was the Lynxmotion *AL5D* (Figure 17) five-degree-of-freedom manipulator with two shoulder, one elbow, and two wrist joints. The arm was controlled by the Logitech *F310 Gaming Gamepad* through the Lynxmotion *RIOS SSC-32* software. Each joint of the arm was controlled by a specific degree of freedom of the controller.

Since the Lynxmotion AL5D arm is not anthropomorphic, the arm motions of the user cannot directly map to the robotic arm, and forward and inverse kinematic solutions were required. The orientation of the user's upper arm and forearm was used to calculate the position of the hand in three-dimensional space. This position was then used to determine the individual joint angles required of the robotic arm. Position and orientation calculations

---

[20] http://www.lynxmotion.com

utilize quaternion mathematics as they avoid issues inherent in other representations such as the gimbal lock problem with Euler angles (Mukundan, 2002).

3.1.1 Participants

Twelve paid participants took part in the study: ten males and two females. All were right-handed. The participants were recruited from the local university community including alumni, graduate students, and undergraduates. Ages ranged from 20 to 40 ($\mu = 28$, $\sigma = 6.6$ yrs). Only two of the participants had regular joystick gaming experience, six had moderate experience, and four had low experience.

3.1.2 Apparatus

The experiment was conducted using the apparatus described previously (Figure 13). Target and error surfaces were constructed from electrically conductive aluminium sheets and connected to input pins on an Arduino *UNO* board with a microcontroller running at 16 MHz . The instrument (replacing Fitts' original stylus) delivered a digital logic level voltage to the surfaces.

The host computer used was an ASUS *Zenbook UX303LN* laptop running at 2.6 GHz with an Intel *Core i7* processor and 8 GB of RAM. Joystick control utilized Lynxmotion's *RIOS SSC-32* software.

The Lynxmotion *AL5D* joystick control hardware communicated with the host computer through a USB 2.0 port at 115200 bits/sec. The control software for the wearable system was developed on Processing, a java-based programming language. Three-dimensional rotation mathematics was implemented through the Toxiclibs Quaternion class in the Processing environment. Another Arduino *UNO* microcontroller controlled the robotic arm for the wearable system. The accelerometer/gyro sensor boards were based on the Invensense *MPU6050* chip running on an 8 MHz Arduino *FIO* host microcontroller. The *MPU6050* refresh rate was set at 25 samples per second. The *FIO* modules communicated wirelessly with the host computer through Digikey *Xbee* radios transmitting in the 900 MHz and 2.4 GHz frequency bands at a data rate of 57600 bits/sec. The *Xbee* receivers connected to the host computer's USB 2.0 and 3.0 ports.

3.1.3 Task and Target Parameters

The reciprocal tapping task consisted of participants touching alternating left and right targets. LED stimulus lights connected to the microcontroller indicated which target to select (see Figure 14). Targets were magnetically mounted to and electrically isolated from the error plate. The software to control the task apparatus was adapted from the FittsTaskOne software from MacKenzie.[21]

There were three target amplitudes *A* = 100 mm, 200 mm, and 400 mm, and three target widths *W* = 24 mm, 48 mm, and 96 mm, giving nine combinations of target widths and amplitudes (Table 1). The *ID*s, described using Equation 2, ranged from 1.03 bits to 4.14 bits. Sessions for each participant consisted of the nine combinations of *A* and *W* organized

[21] http://www.yorku.ca/mack/FittsLawSoftware/

in sequences of 20 trials, with nine sequences covering the $A \times W$ conditions. Movement times of the instrument between targets and errors were recorded for each trial.

3.1.4 Procedure

The participants were introduced to the experimental task for each of the three control modes. For sessions with the robotic arm, the participants were seated in a comfortable position behind both the arm and the apparatus. They were then instructed to position themselves for an optimal direct view of the target area. For the manual target selection method, seating was directly behind the apparatus within arm's reach. Each participant was given 20 practice trials with each control mode. Before each session, participants rated their level of physical comfort. After the session they again rated their comfort level. At the end of the study, the participants completed a questionnaire with ratings for mental effort, physical comfort, and ease of use for each control mode.

There were two phases of calibration for the accelerometer and gyro sensors. Before the experiment began each sensor had an initial calibration phase lasting roughly ten seconds. Although not reported in the documentation, this auto calibration has been observed during initial experimentation with the sensor. During power up the sensors were placed with the positive Y axis pointed towards the screen plane and the positive Z axis pointing upwards opposite the gravity vector of the Earth. The subsequent phases of calibration occur throughout the experiment after each sequence of thirteen trials. Participants were asked to place their right arms straight down by their sides and the quaternion offset was determined and applied to subsequent motion calculations.

3.1.5 Design

The experiment used a within-subjects design with the following independent variables and levels:

Independent Variable	Levels
Control mode	User Arm, Joystick, Wearable
Target Amplitude	100 mm, 200 mm, 400 mm
Target Width	24 mm, 48 mm, 96 mm

Table 1: Experiment 1 independent variables and levels.

Participants were assigned to groups with control modes counterbalanced using a Latin square. The test software randomized the target widths and amplitudes within each control mode. The dependent variables were movement time, error rate, and throughput. A threshold of a 40% error rate was set to trigger a repeat of a block of trials, but no participant exceeded the threshold. The duration of the experiments was roughly one-and-a-half hours per participant. For each participant there were 3 control modes × 3 amplitudes × 3 widths × 20 trials for a total of 2700 trials.

3.2 Results

The mean throughputs for the user arm, joystick, and wearable control modes were 5.58 bits/s, 0.74 bits/s, and 0.80 bits/s, respectively (Figure 18). An ANOVA of the results indicated significant differences in the throughputs by control mode ($F_{2,11} = 158.77$, $p < .0001$). A post hoc analysis indicated significant differences for the user arm versus joystick, and user arm versus wearable, but no significant difference between the joystick and wearable methods. Throughputs were calculated as per the ISO 9241-9 specification using the discrete error method to calculate ID_e values.

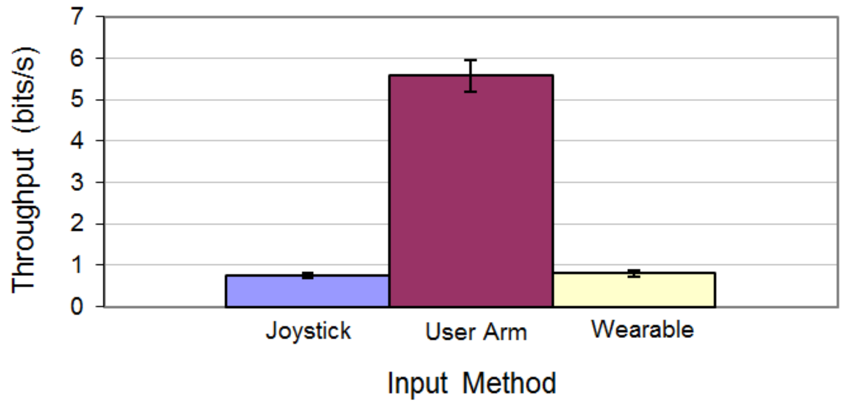

Figure 18: Throughput by control mode. Error bars show ±1 *SE*.

The mean movement times for the user arm, joystick, and wearable methods were 440 ms, 3235 ms, and 2983 ms, respectively (Figure 19). An ANOVA indicated significant differences in mean movement time by control mode ($F_{2,11} = 63.43$, $p < .0001$). A post hoc analysis indicated significant differences for the user arm versus joystick methods, and the user arm versus the wearable, but no significant difference between the joystick versus the wearable method.

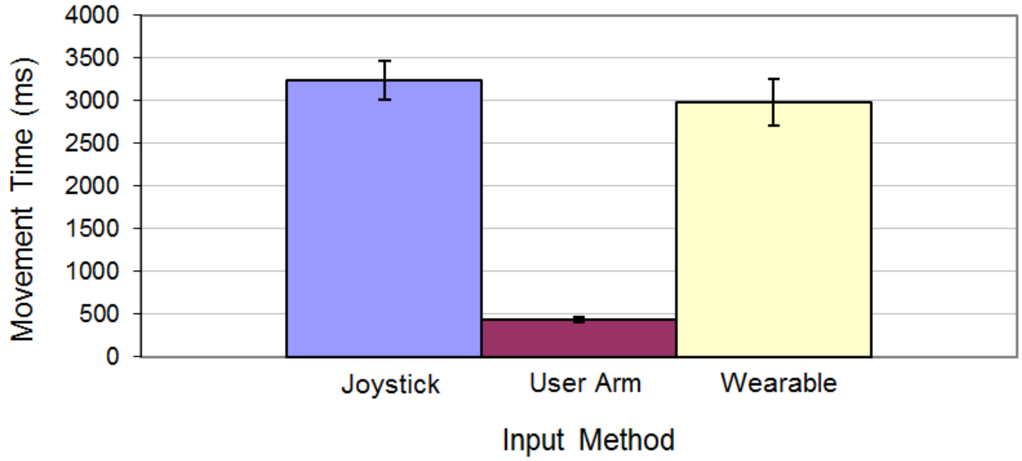

Figure 19: Movement time by control mode. Error bars show ±1 *SE*.

The mean error rates for the user arm, joystick control of the robot arm, and wearable control of the robot arm were 0.89%, 4.11%, and 8.44%, respectively. See Figure 20. An ANOVA indicated significant differences in the mean error rate by control mode. ($F_{2,11}$ = 10.42, p < .0001). A post hoc analysis revealed significant differences in the error rates between all three pairwise combinations (p < .05).

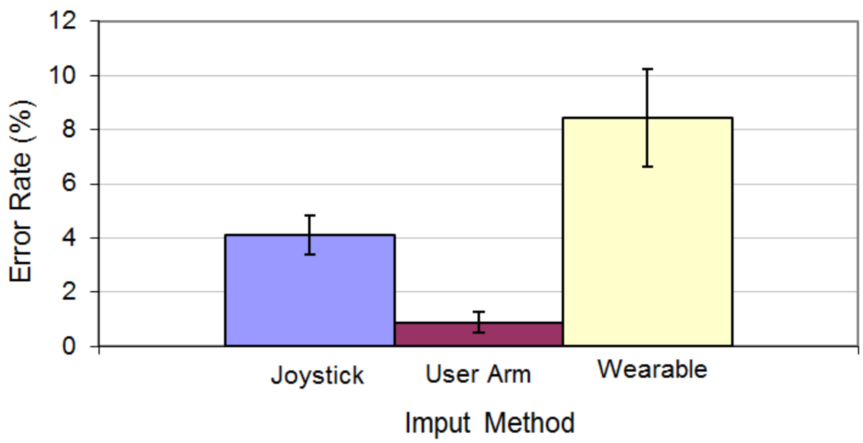

Figure 20: Error rate by control mode. Error bars show ±1 *SE*.

Participants were asked to rate their subjective feelings with each control mode. Responses were solicited on a 5-point Likert scale for "comfort", "effort" and "ease of use". See Table 2.

Participant	Comfort			Effort			Ease of Use		
	Joystick	User Arm	Wearable	Joystick	User Arm	Wearable	Joystick	User Arm	Wearable
P1	5	4	3	4	1	3	3	5	4
P2	4	5	2	4	1	3	3	5	4
P3	4	4	3	2	3	3	4	5	3
P4	5	5	3	4	1	3	2	5	3
P5	4	5	4	1	1	2	5	5	3
P6	5	5	4	2	1	3	4	5	3
P7	5	5	4	5	1	4	3	5	4
P8	4	5	3	3	1	2	3	5	3
P9	5	5	4	2	1	4	5	5	4
P10	4	5	3	2	1	3	4	5	4
P11	4	5	4	3	1	2	3	5	4
P12	4	5	5	2	1	2	4	5	3
Mean	4.42	4.83	3.50	2.83	1.17	2.83	3.58	5.00	3.50
SE	0.15	0.11	0.23	0.34	0.17	0.21	0.26	0.00	0.15

Table 2: Comfort, effort, and ease use ratings for experiment 1.

For "comfort" , the responses ranged from 1 = very uncomfortable to 5 = very comfortable. As seen in Figure 21 and as expected, participants found their own arm the most comfortable (4.83), followed by the joystick (4.42), and lastly the wearable method (3.50). A Friedman non-parametric test deemed the differences statistically significant ($H_2 = 15.7$, $p < .0005$). Pairwise comparisons using Conover's F revealed significant differences between all three pairs of control modes ($p < .05$).

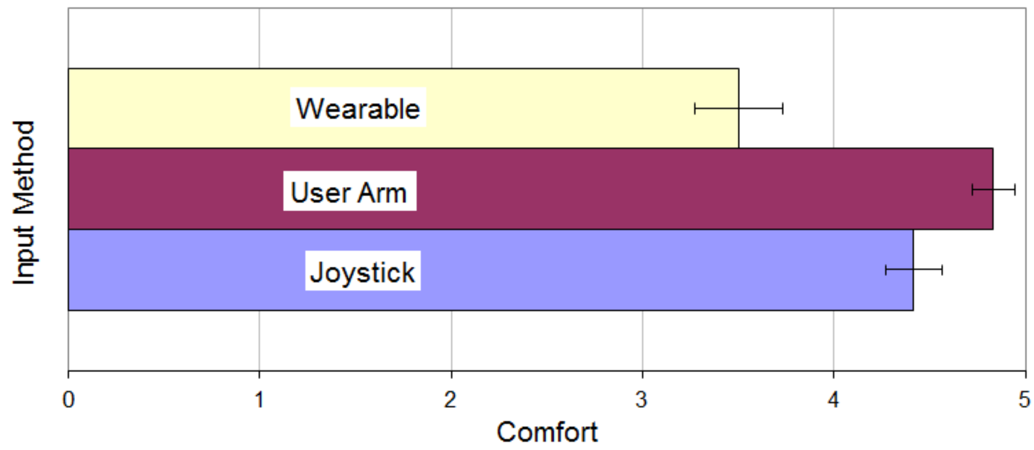

Figure 21: Comfort level. Higher scores are better. Error bars shows ±1 *SE*.

The three control modes were similarly rated by the participants for "ease of use" (Figure 22). The participants unanimously rate use of their own arm easy to use (5.0). The wearable and joystick control modes received ratings similar to one another (3.50 and 3.58, respectively). See Figure 22. The differences in ratings were statistically significant (H_2 = 15.15, $p < .001$) with significant pairwise differences for the joystick + user arm and wearable + user arm pairings.

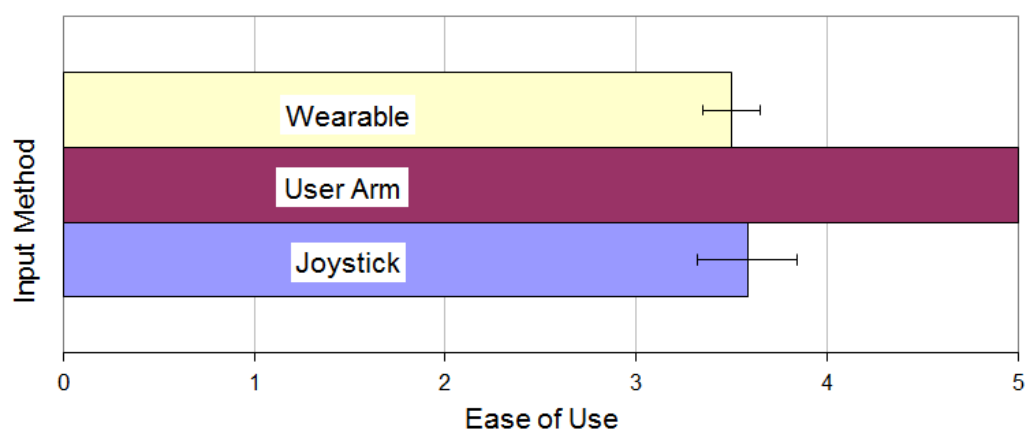

Figure 22: Ease of use. Higher scores are better. Error bars shows ±1 *SE*.

For "effort" the results were similar, except noting that lower scores are better (1 = very low effort, 5 = very high effort). See Figure 23. The best (i.e., lowest) score was for the user arm control mode (1.17), followed by the wearable and joystick control modes which received the same mean rating (2.83). The differences were statistically significant (H_2 = 12.5, p < .005) again with significant paired differences between the user arm and wearable condition and the user arm and joystick condition.

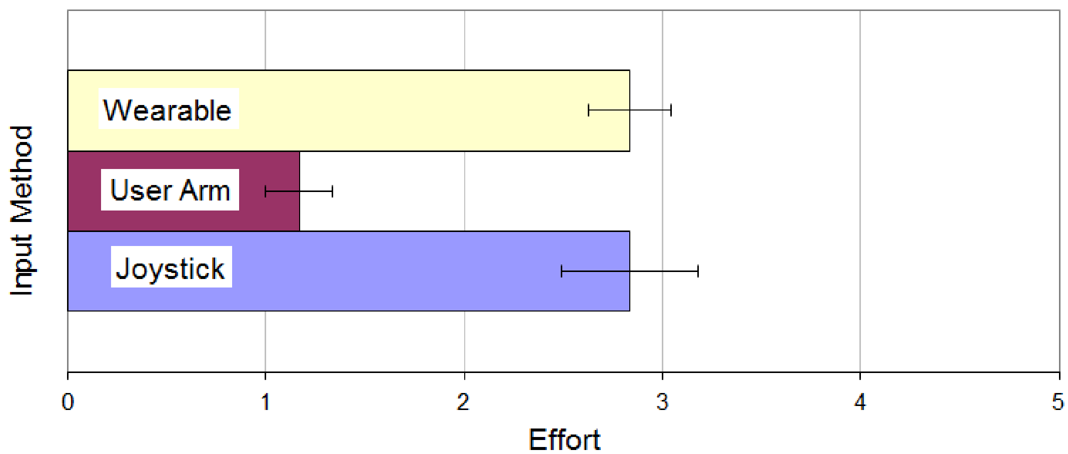

Figure 23: Effort level. Lower scores are better. Error bars show ±1 *SE*.

Table 3 summarizes the quantitative results for the first experiment on each of the three dependent variables.

Control mode	Movement Time (ms)	Error Rate (%)	Throughput (bits/s)
Joystick	3235	4.11	0.74
User Arm	440	0.89	5.58
Wearable	2983	8.44	0.80

Table 3: Grand means for joystick, user arm, and wearable control modes.

3.2 Discussion

The results for the throughput of both our wearable system and joystick methods are low compared to the results from similar teleoperation studies (Table 4). Our throughput was 0.80 bits/s with the wearable system and 0.74 bit/s for the joystick. This is in contrast to values of to 2.00 bits/s, 2.88 bits/s and 1.49 bits/s from Mihelj et al. with the IRB-6, and Draper et al. (1990), and Draper and Handel (1989) respectively with the ASM. Results for throughput of the user arm condition of the Fitts' reciprocal tapping task were 5.58 bits/s for our study and 14 bits/s, 16.98 bits/s and 11.27 bits/s from the others (Table 1). The throughputs for the user arms in the other studies were much greater but were not calculated as per ISO 9241-9 and not directly comparable to our results. Our throughput calculations used the discrete error method to determine the effective Index of Difficulty rather than the presented values. The motivation for this was to determine the participants' actual task performance rather than what was expected.

We also considered the ratios of the performance in throughput (*TP*) of the user arm over the teleoperated systems as another method of comparing performance, since we can compare within our participant pool rather than between pools. Comparing these ratios we obtain 6.95 for our wearable system, 7.55 for the joystick, and 7.00, 5.90 and 7.56 for various devices from the other studies. See Table 4. These ratios are roughly in the same range. However, we are reminded that each of the teleoperated systems differ in the method of control; from the wearable and joystick methods of our study, to the camera tracking system, and the master replica/slave system of the others.

Study	Device	TP (bits/s)	(Arm TP / Manipulator TP)
Young, 2016	Wearable	0.80	6.95
	Joystick	0.74	7.55
	User Arm	5.58	-
Mihelj et al., 1998	IRB-6	2.00	7.00
	User Arm	14.00	-
Draper & Handel, 1989	ASM	1.49	7.56
	User Arm	11.27	-
Draper et al., 1990	ASM	2.88	5.90
	User Arm	16.98	-

Table 4: Throughputs for user arm and telemanipulator system comparison

Our results show no significant differences in the joystick versus wearable control modes in measures of throughput, movement time, and error rate. This is somewhat surprising as the control modes vary significantly in a number of ways. The wearable method employs a one-to-one mapping of the position of the participant's hand to the end effecter in real three-dimensional space. While the joystick is a position control device there is no such mapping. The velocity limits of the end effector were not measured so it is not known whether the system is operator-paced or machine-paced. The input frequency of our wearable accelerometer/gyro system is set at 25 Hz which is well above the 0.64 Hz limit for machine-pacing determined by Draper and Handel (1989). Wireless communications from the sensors are set at 57600 baud and communication to the manipulator servo controller from the host computer is set at 115200 baud, well above operator pacing requirements. The joystick method communicates with the manipulator servo controller also at 115200 baud.

Another possible factor is the speed of controller movements. In our wearable method, movements occur at the shoulder and elbow joints of the participant's arm, and these movements map out a one-to-one positioning of the participant's hand to the end effector. With the joystick, because there is no one to one mapping, only small motions of the human thumbs are required. The throughputs of these joints are well within the capability of both our wearable system and the manipulator system to handle. It should be noted that the joystick method requires two arms and hands, whereas the wearable method only requires one arm.

However, while the system is capable of handling the input frequencies, the overall system lag is another consideration. MacKenzie and Ware (1993) have demonstrated that movement times and error rates increase with system lag. These results were also supported by Teather et al. in their study of latency and jitter. It is possible that latency in the joystick control mode is different from the wearable method since the hardware is different. We implemented our own servo motor control for the wearable input system. The joystick input utilized Lynxmotion's servo controllers. The wearable control mode requires one additional layer of processing on the host computer before control commands are sent to the servo motor controller. This layer of processing involves wireless communications from the accelerometer/gyro sensors to the host computer where raw quaternion data is processed and transformed through inverse kinematics into control data which is then sent to our servo motor controller system. The lag introduced by this additional layer of communications and data processing is unknown but may be a factor in our human performance measures.

In comparing the throughputs of our teleoperated system with those in the studies mentioned previously, we note that a direct comparison is not valid since the control modes differ. Also it is unknown whether these systems were either operator-paced or machine-paced through either human input frequency or end effecter velocity. For the purposes of our study, we wish to only compare the performance of our wearable method with the joystick.

The error rate for the wearable method was almost twice as high as that of the joystick control. This is understandable since the wearable method required unsupported arm motions which are physically demanding and fatiguing. Users are more prone to errors when experiencing discomfort. Unsurprisingly, the wearable method was rated as the most uncomfortable. The user's arm had the lowest error rate which is to be expected since the task is direct rather than displaced, and the view of the task area was also direct rather than displaced and visually occluded by the robotic arm in the joystick and wearable tasks.

The participant ratings of comfort for control mode are expected. Participants using their own arm and the joystick to perform the reciprocal tapping task experienced no significant discomfort. The wearable method however induced significant discomfort since the arm was unsupported. Note that while mechanically both the user arm and wearable control modes should be identical – because of the one-to-one mapping of the end effector to the hand position – they are not. In performing the task manually using their own arms, participants can rest their elbows on the table as a supporting surface and thus need only to pivot their forearms. Because of the separation from the task area by the telemanipulator, the participant movements are in air and unsupported. It should be noted as well that during the trials with the joystick and wearable control modes, the telemanipulator partially occluded the participants' view of the task area. With the manual Fitts' task using their own arms, the participants had a direct view of the task area. A number of previous studies utilized complex camera and monitor setups for their teleoperator trials.

In terms of effort, participants unsurprisingly rated using their own arms as the easiest. There were no significant differences in effort level between the joystick and wearable methods. In this particular study, the Fitts' reciprocal tapping task is one-dimensional so there is little cognitive demand for using the joystick. Participants simply needed to raise and lower the end effector with one motion while performing a translation with another. The mental process required in achieving the goal and performing the task is to map the desired motions of the end effector to finger movements controlling the joystick. Contrary to the joystick there should be no need for mentally mapping motions of the human arm for the wearable method. Thus, ideally, the effort level required should be less than that of the joystick. It should be noted that, although Fitts' reciprocal tapping task is one-dimensional, there are two dimensions to the task since the stylus must be lifted up to move between target plates. A one-dimensional movement of the stylus will cause a hit on the error plane. It is likely though that the participants easily adapted to the two-dimensional nature of the task since the standard computer control (the mouse) and display is two-dimensional. In a three-dimensional task, the cognitive mapping to the joystick may require more mental effort.

Again with the overall ease of use, the participants rated their own arms the best while there was no significant difference between the joystick and wearable control modes. Given that the effort level was not significantly different between the joystick and wearable methods and that the wearable method induced significant discomfort, the ease of use should have been rated lower for the latter. Perhaps the participants did not factor in the discomfort or did not consider the discomfort to be significant.

CHAPTER 4 - EXPERIMENT 2

4.1 Methodology

For the second experiment, a three-dimensional Fitts' reciprocal tapping task was implemented in fish tank VR. The experiment used our wearable system for target selection on a computer screen. Movement times, error rates, throughputs were measured for three different target selection methods: a baseline button click with a handheld ergonomic controller, dwell time (MacKenzie and Teather, 2012), and a novel twist gesture (Figure 24). For the dwell time method, the target cursor must enter the target volume and stay within that volume for a prescribed time period after which a selection event occurs. A study examining dwell time determined that 350 to 600 ms felt neither too fast nor too slow for subjects (Müller-Tomfelde, 2007), thus we chose 500 ms. The dwell time imposes an upper limit on performance in terms of movement time and throughput.

For the twist selection gesture, the user must move the cursor within the target volume, then rotate their hand along the longitudinal axis to generate a selection event. This gesture is performed by supination of the wrist and forearm for right handed users in our study. We defined (following pilot testing) a threshold of a 40 degree rotation clockwise in less than 100 milliseconds to generate a selection event. The dwell time and twist gesture methods were chosen while accelerometer/gyroscopes are ubiquitous in modern devices, these devices do not always have convenient buttons available and would necessitate holding another device in a hand such as our ergonomic controller for the baseline click task.

Participants wore stereoscopic 3D glasses to generate the illusion of depth in the displayed fish tank virtual reality screen, and selected targets on a 3D monitor. The dimensions of the "fish tank" were 30 cm in the perceived depth into the monitor, 29 cm from top to bottom, and 51 cm across the width of the screen. Target volumes were placed at depth of 0 cm, 5 cm, and 10 cm "into" the screen.

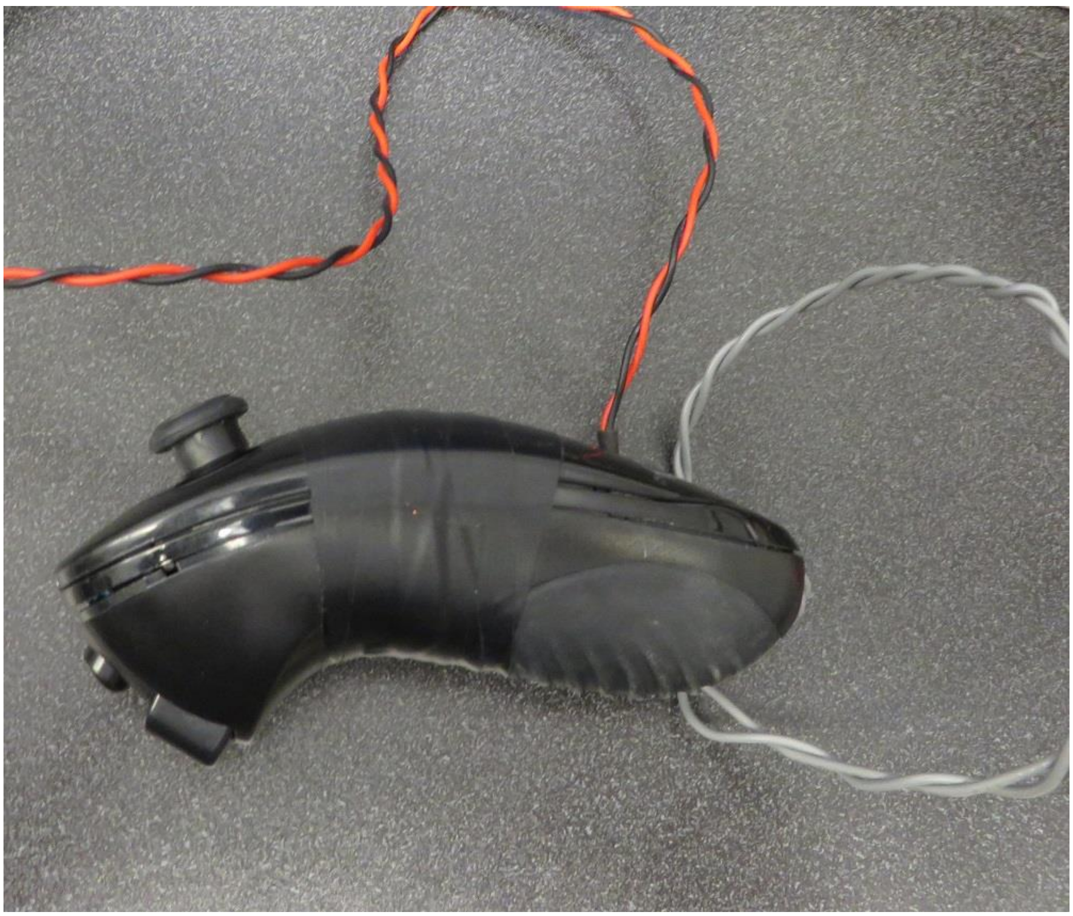

Figure 24: Ergonomic button click controller.[22]

[22] Young, T. (Photographer). 2015.

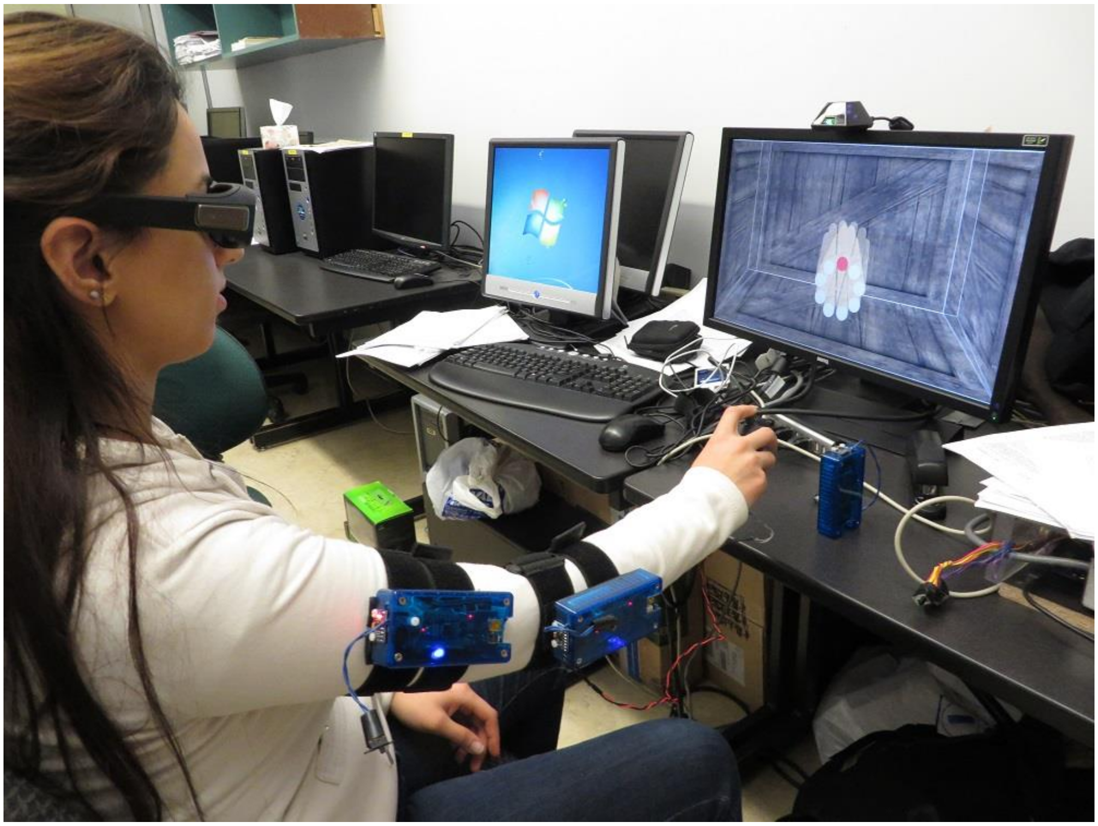

Figure 25: Click method.[23]

[23] Young, T. (Photographer). 2015.

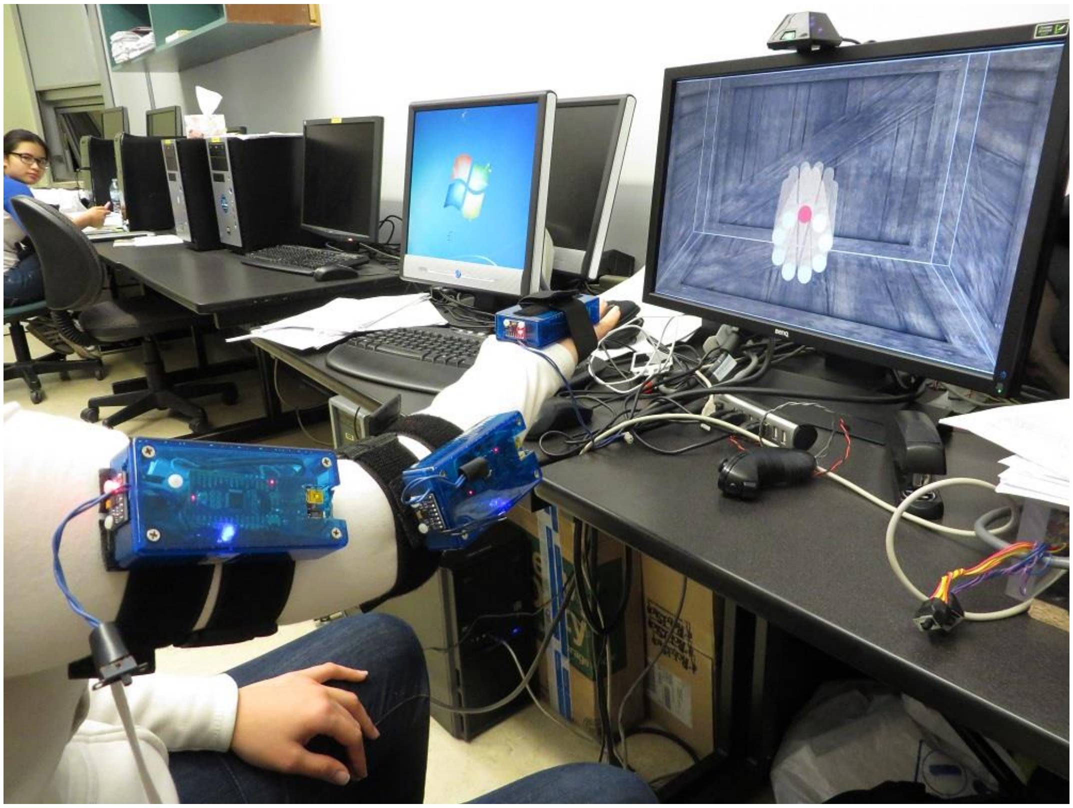

Figure 26: Twist method.[24]

A pilot study was initially conducted with eight participants. A CD gain of 1.5 was set for motion in planes parallel to the screen plane, and a gain of 4 was set for motion in the depth direction. Participants performed twenty-seven sequences of nine trials each without rest. Each trial consisted of selecting targets in a Fitts' reciprocal tapping task.

4.1.1 Participants

Twelve participants were recruited from the local university community including current undergraduate and graduate students and alumni. There were four females and eight males.

---

[24] Young, T. (Photographer). 2015.

Ages ranged from 29 to 40 (μ = 25.8, σ = 5.1 yrs). Of the participants, three had moderate experience with 3D controllers, three had low experience, and six had no experience. All the participants had normal stereo acuity and all were right handed.

4.1.2 Apparatus

The apparatus for the wearable system was the same as used in Experiment 1. The stereoscopic 3D glasses were the NVIDIA *3D Vision 2 Wireless Glasses* with LCD shutters. The host computer configuration consisted of an AMD *Athlon II X4 635* processor running at 2.90 GHz with 4.00 GB RAM, a Microsoft 64 bit *Windows 7 Enterprise SP1* operating system, and an NVIDIA *GTX 560 TI* video card. The display monitor was a BenQ *XL240T* running at 120 Hz. The click selection method utilized a modified ergonomic handheld controller with the switch connected to a digital input on one of our inertial devices (Figure 24). The twist selection method included a third inertial device worn on the hand to detect rotation about its roll axis. No extra hardware was needed for the dwell selection method. A three-dimensional cursor of the jack type was used for the selection tool (Figure 27).

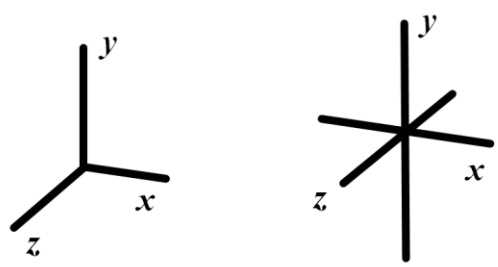

Figure 27: 3D cursors skitter (left) jack (right).

4.1.3 Target Parameters

The reciprocal tapping task consisted of participants selecting thirteen targets arranged in a circle (Figure 28). The target to select was highlighted in red and turned blue when the cursor entered the target. Note that the targets were spheres although they appeared to be circles. The software to control the task was a modified version from Teather and Stuerzlinger (2013).

Figure 28: Fitts' 3D task.[25]

[25] Young, T. (Photographer). 2015.

There were three target amplitudes A = 3.5 cm, 5.5 cm, and 7.5 cm, three target diameters W = 0.5 cm, 0.75 cm, and 1.0 cm, and three target depths D = 0 cm (at screen depth), -5.0 cm, and -10.0 cm (behind the screen) giving 27 combinations of target diameters, amplitudes and depths. The presented *ID*s, described in Equation 2, ranged from 2.17 bits to 4.00 bits. Sessions for each participant consisted of the 27 combinations of A, W and D organized in sequences of 12 trials (13 targets). Movement times of the cursor between targets and errors were recorded for each trial.

4.1.4 Procedure

The participants were introduced to the experimental task for each of the three target selection methods. For each session, participants were seated in a comfortable position away from the target surface with enough room to move their arms. Each participant was given roughly two to five minutes of practice with each selection control mode and to assess normal stereo acuity. They were also instructed to maximize both movement speed and precision. After each control mode, participants rated their level of physical comfort. At the end of the study, the participants completed a questionnaire with ratings for mental effort, physical comfort, and ease of use for each selection method.

4.1.5 Design

The experiment used a within-subjects design with the following independent variables and levels:

Independent Variable	Levels
Selection Method	Click, Dwell, Twist (Figure 24)
Target Amplitude	35 mm, 55 mm, 75 mm
Target Diameter	5 mm, 7.5 mm, 10 mm
Target Depth:	0 mm, -50 mm, -100 mm

Table 5: Experiment 2 independent variables and levels.

Participants were divided into groups with selection method counterbalanced using a Latin square. The software randomized the amplitude, diameter, and depth values within each control mode. The dependent variables were movement time, error rate, and throughput. The duration of the experiment was roughly 1.5 hours per participant. For each participant there were 3 selection methods × 3 amplitudes × 3 widths × 3 depths × 12 trials for a total of 972 trials. This yielded 11,664 trials over twelve participants.

4.2 Results

The mean movement times for the click, dwell, and twist selection methods were 3514 ms, 3499 ms, and 3327 ms, respectively (Figure 29). An ANOVA of the results indicated no significant differences in the movement time by selection method ($F_{2,11} = 1.065$, $p > .05$).

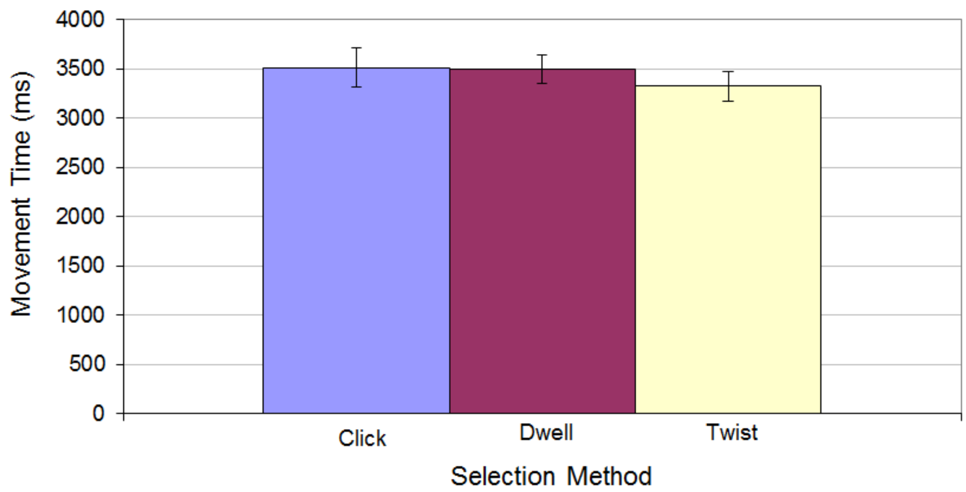

Figure 29: Movement time by selection method. Error bars show ±1 *SE*.

The mean error rates for the click, dwell, and twist selection methods were 6.82%, 0.00%, and 3.59%, respectively (Figure 30). An ANOVA indicated significant differences in the mean error rate by selection method ($F_{2,11}$ = 28.70, p < .0001). A post hoc analysis revealed significant differences in the error rates between all three pairs of selection methods.

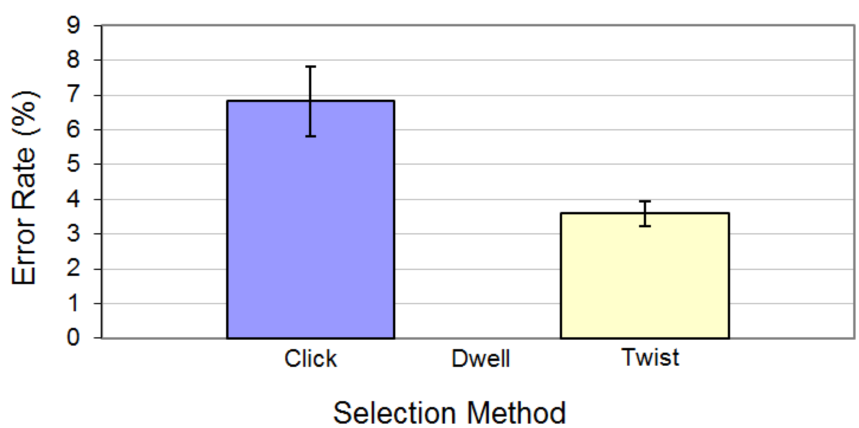

Figure 30: Error rate by selection method. Error bars show ±1 *SE*.

The mean throughputs for the click, dwell, and twist selection methods were 0.94 bits/s, 0.95 bits/s, and 0.89 bits/s, respectively (Figure 32). An ANOVA of the results indicated no significant differences in the throughputs by selection method ($F_{2,11} = 1.48$, $p > .05$). The throughputs were calculated as per the ISO 9241-9 specification using ID_e rather than ID. The effective distance and width in three dimensions was calculated by projecting the vector of movement along the target axis and determining the overshoots and undershoots from the Cartesian distance between the origin and target coordinates (Teather, 2013).

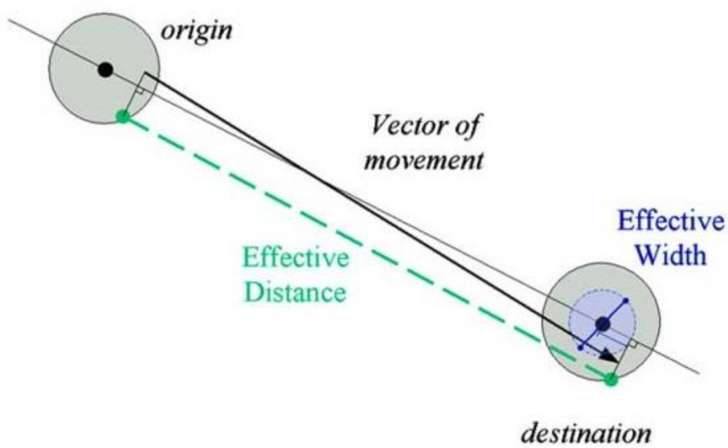

Figure 31: Calculating the effective index of difficulty (ID_e).[26]

[26] Teather 2013.

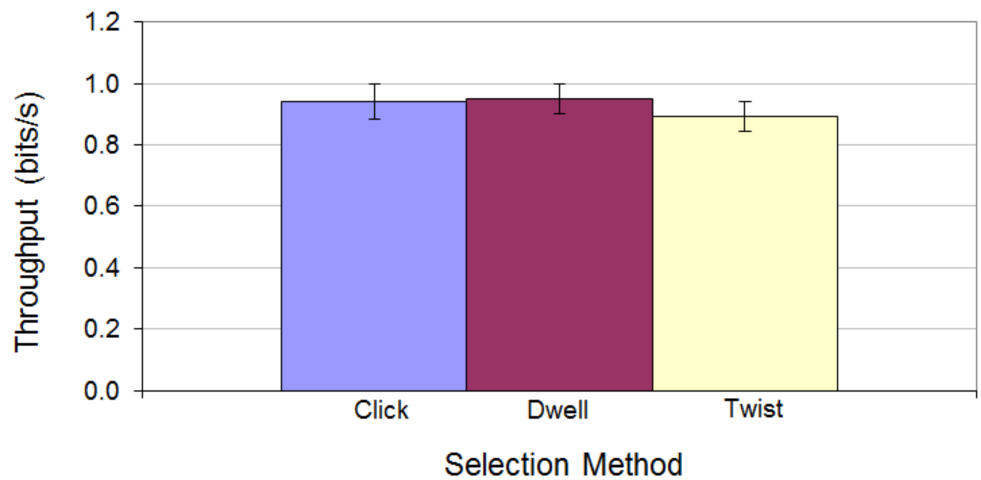

Figure 32: Throughput by selection method. Error bars show ±1 *SE*.

As with Experiment 1, participants were asked to rate their subjective feelings for each selection method. Responses were solicited for "comfort", "effort" and overall "preference" of selection method. See Table 2.

Participant	Comfort			Effort			Preference		
	Click	Dwell	Twist	Click	Dwell	Twist	Click	Dwell	Twist
P1	5	5	5	5	4	3	5	4	4
P2	1	4	2	4	3	2	4	2	2
P3	3	3	4	3	4	4	2	3	4
P4	3	4	3	3	4	2	3	4	2
P5	5	2	3	3	2	4	3	2	4
P6	3	4	3	3	5	4	3	5	2
P7	2	3	3	3	2	2	3	4	4
P8	3	2	4	2	5	1	3	5	3
P9	4	2	3	4	1	4	5	1	4
P10	4	4	4	3	4	5	3	3	4
P11	4	4	4	4	3	5	4	3	5
P12	4	3	3	4	4	4	5	4	3
Mean	3.42	3.33	3.42	3.42	3.42	3.33	3.58	3.33	3.42
SE	0.36	0.31	0.25	0.24	0.39	0.41	0.28	0.38	0.31

Table 6: Comfort, effort and preference ratings for experiment 2.

For "comfort", a Friedman non-parametric test revealed that the differences in the responses across the three selection methods was not statistically significant (H_2 = 0.125, p > .05). The response were narrowly clustered at about 3.3. See Figure 33.

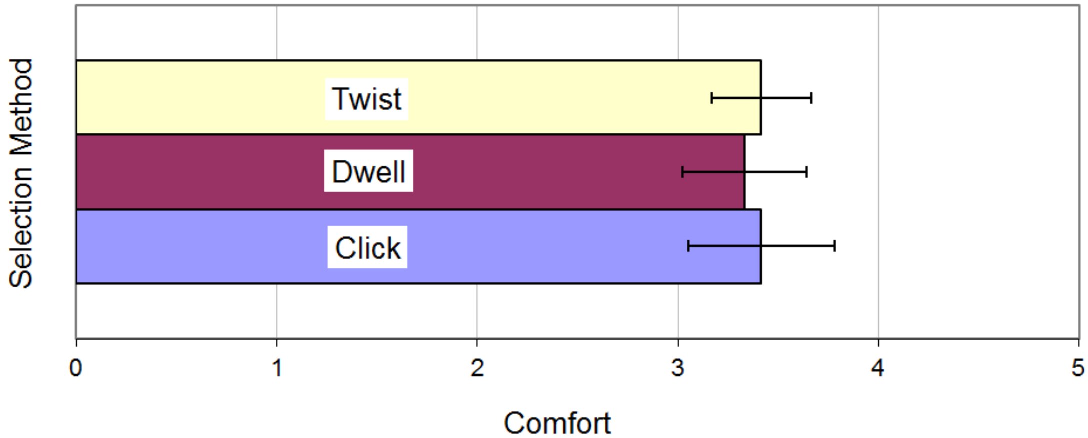

Figure 33: Comfort level by selection method. Higher scores are better. Error bars show ±1 *SE*.

The overall level of effort, both mental and physical, for each selection method was rated by the participants. The response means were 3.33 (twist), 3.42 (dwell), and 3.42 (click). See Figure 34. The differences were not statistically significant (H_2 = 0.04, p > .05).

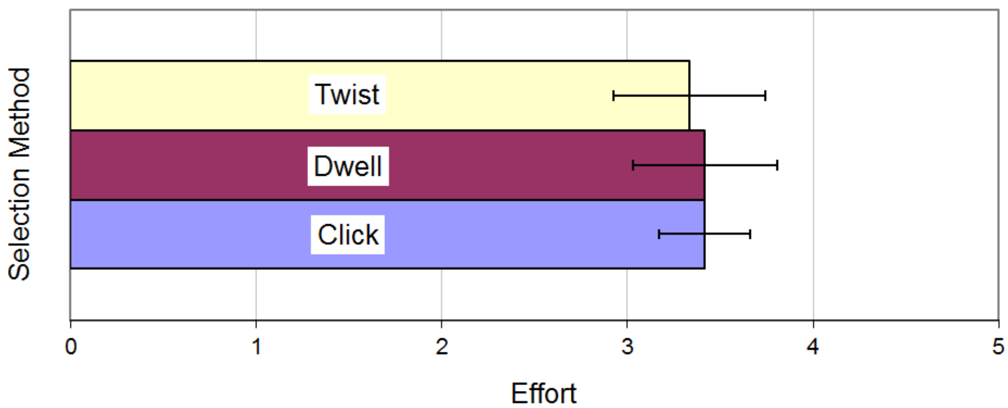

Figure 34: Effort level by selection method. Higher scores are better.

Error bars show ±1. *SE*.

The overall preference, for each selection method was rated by the participants, as shown in Figure 35. The response means were 3.42 (twist), 3.33 (dwell), and 3.58 (click). Again, the differences were not statistically significant (H_2 = 0.17, p > .05).

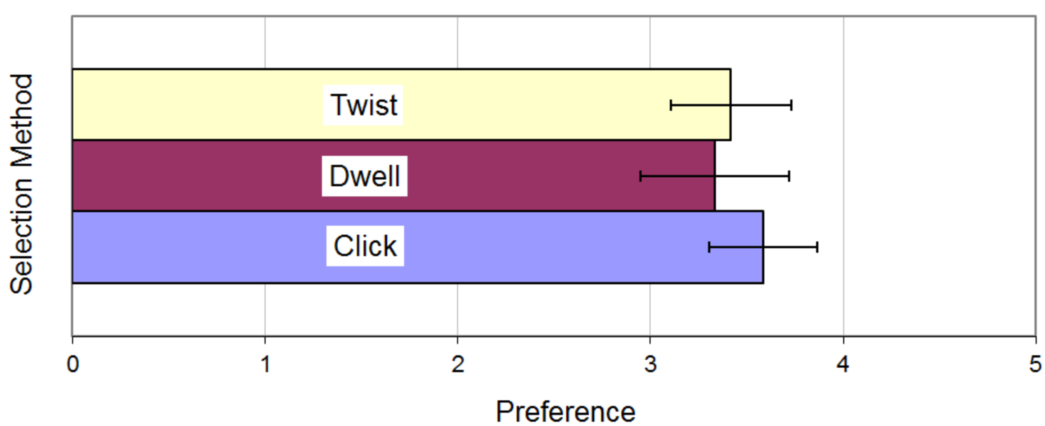

Figure 35: Preference by selection method. Higher scores are better.

Error bars show ±1 *SE*.

Table 7 summarizes the quantitative results for the second experiment on each of the three dependent variables.

Selection Method	Movement Time (ms)	Error Rate (%)	Throughput (bits/s)
Click	3514	6.82	0.94
Dwell	3499	0.00	0.95
Twist	3327	3.59	0.89

Table 7: Grand means for click, dwell, and twist selection methods.

4.3 Discussion

In-air unsupported pointing is a physically demanding task. It was observed that, over time, participants experienced increasing levels of fatigue and both error rates and movement times increased. Each block of trials consisted of 324 target selections. During the pilot study for this experiment, very few participants were able to consecutively perform all 27 sequences (9 trials per sequence). Fewer achieved acceptable error rates which sometimes approached 50% in some sequences. The experiment parameters were changed in view of the pilot study, as now described.

The pilot study used a CD gain of 1.5 in the task axis parallel to the screen plane, and a gain of 4 in the depth axis. The initial motivation was to mitigate fatigue by requiring less arm motion, however because of the constant gain, as opposed to pointer acceleration, it was observed that participants tended to overshoot targets and spend more time correcting. This effect became more pronounced over time. Another factor was the positioning of the targets. At first they were set at a lower height so that participants would only have to raise their arms minimally to mitigate fatigue. This became a problem in their seated positions as the participants' legs would interfere with arm movements when attempting to reach lower targets.

For the final experiment we settled on a CD gain of 1.25. This provided a reasonable balance between fatigue reduction and error. Additionally, on the thirteenth target (used as a dummy value), participants were encouraged to rest for a period of ten to twenty seconds. This rest greatly mitigated the fatigue of the participants and all were able to complete the study with minimal errors.

For cursor movement, there was a direct mapping of real world coordinates to the virtual screen position. Cursor or pointer acceleration functions, such as those designed to maximize precision, were not implemented. It was observed that participants were initially not able to easily reach the targets. Although the stereo depth cues help provide some notion of three dimensions, many participants moved their arms initially not understanding that the trajectory of the cursor in three dimensions follows an arc rather than straight lines.

Although the throughput values in Figure 32 are low, values under 1.0 bit/s have been reported in the literature previously (Teather and Mackenzie, 2014: MacKenzie and Oniszczak, 1998: Magee et al, 2015).

There were no significant differences in the movement times and throughputs for all three selection methods. Moving the cursor between targets requires the same motions consisting of a ballistic phase and a corrective phase. However, there should have been some difference between the dwell method and the click and twist method. The end of a trial is signified by the target selection condition, either a button click, a twist gesture, or a dwell time threshold. The total time for a trial is the sum of the travel time, defined as the time from the previous selection event to the time the cursor reaches its final destination, plus the time required for the new selection event. With the dwell method, the time threshold was set to an optimal value 500 ms determined in the previous literature. It was expected that this additional delay should have appeared in movement time results, but it did not. This suggests that there are other factors more significant than the dwell time at play.

Error rates between all three methods were significant. This is unsurprising since the dwell method requires the cursor to be within the target to initiate the timer for a selection event. Thus by definition, the error rate must be zero. If the cursor left the target before the end of the timer countdown then the whole process would need to be repeated. The twist method was implemented with a "sticky" function. This was necessary because of the "Heisenberg Effect" (Bowman et al., 2002). Without the sticky function, users who attempted the twist motion tended to move the cursor outside of the target volume thus resulting in an error for all but the largest of target sizes. The sticky function allows the cursor to stay fixed during twist detection. The stickiness of the target most likely contributed to lower error rates. The Heisenberg effect applies as well to the button click method, however only the motion of one finger is required as opposed to the whole hand required in the twist method. The action of clicking the button on the ergonomic controller does not displace the cursor beyond the target volume.

It is unsurprising that no significant differences were found for the means of the throughputs of the various selection methods. Again the same arguments for movement time apply to throughput. Both the ballistics phase and the correction phase are the same in all of the methods. Determination of ID_e does not vary since the statistical distribution of overshoots and undershoots in cursor hit positions along the target axis is independent of the selection method. As observed previously, the dwell time of 500 ms, yielded no significant difference in movement time, so this does not influence throughput.

There were no significant differences in the scores assigned to comfort in any of the three selection methods, nor did post hoc analysis reveal any pair wise differences. This is to be expected given that the arm motion moving from one target to the next is the dominating factor in each trial movement. The comfort required to either click a button, dwell within a target, or perform a twist gesture of the wrist makes minimal impact on comfort since each action is only momentary, almost immediately for click, 500 ms for dwell, and within 100 ms for the twist method. Compared to the movement times on the order of 2 to 4 seconds, these selection times are minimal in terms of potential fatigue and discomfort.

No significant differences were found in the effort required for each selection method. Some participants reported that they found the dwell method the most taxing since they were required to keep the cursor within the target volume for 500 ms. Others felt that the twist method was easier since the sticky function helped keep the cursor steady for the duration of the gesture. Three participants improperly performed the twist gesture by bending their wrists while moving the cursor between targets (Figure 37). By bending the wrist then performing the twist gesture, the rotation was no longer measured on the longitudinal axis of the hand, but rather at an awkward angle. Thus they were unable to complete the requirements of the rotation, 40 degrees within 100 ms. Some participants had to perform the twist twice or more to successfully generate a selection event.

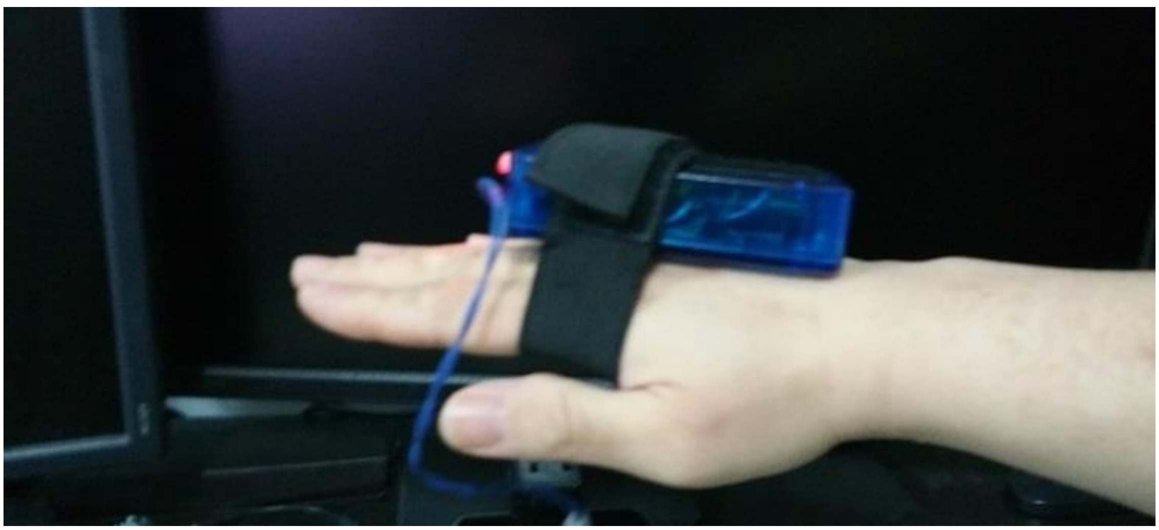

Figure 36: Correct orientation for twist method.

Figure 37: Incorrect orientation for twist method.

Overall the participants did not express strong preferences for any of the selection methods. No significant differences were found in the scores assigned. One participant expressed extreme dislike for the dwell method, rating it the lowest possible score, while two others rated dwell at the highest level. Three participants rated click as the most preferred method. This is understandable since it is the de facto method of selection and probably the most familiar for gamers.

There were a number of issues in the experimental setup that warrant discussion. As discussed previously, the CD gain settings were chosen to maximize comfort and performance. However, another important factor is the physical location of the work area displayed in real world coordinates. Because this system uses the virtual hand or depth cursor metaphor, the onscreen cursor mimics the motion and position of the user's real hand. Thus the participants in the study found that their real hand visually occluded the onscreen targets in certain circumstances. Offsetting the location of the work area either upwards or downwards was problematic. If the arm motions were vertically offset lower, the user would have to compensate by moving their arms higher, thus causing more fatigue and discomfort. A higher offset was problematic as users had to compensate by moving their arms lower. Because the users were seated this meant that their arms would come into contact with their legs as they tried to reach the lower targets onscreen. Thus, proper gain settings and height offsets had to be chosen carefully to avoid these problems. As previously discussed, if the CD gain settings were increased such that relatively small angular displacements of the user's arm resulted in large cursor movements onscreen, then accuracy and error rates would suffer. This issue could be dealt with by implementing an acceleration function similar to Microsoft Windows' mouse acceleration. A seated position at a desk may not be the optimal environment or application for our wearable system. A large high resolution display or a CAVE where users stand up may be a more suitable application.

CHAPTER 5 - DISCUSSION

5.1 The Wearable System

Although our wearable system utilizes six degree of freedom sensors, our experiments only require three, the coordinates of our virtual hand in three dimensional space in the world reference in Experiment 1, and in virtual 3D space in Experiment 2. Because of this, we cannot test the full capabilities of our system. Applications requiring pose information (both location as well as orientation) such as CAD/CAM, or surgical robotics, would perhaps be better suited for our wearable method. As mentioned previously, the cognitive demand of an essentially one dimensional task, our Experiment 1 reproducing Fitts' original experiment, is relatively low compared to tasks which require more degrees of freedom. Given that, it is understandable why the joystick performs as well as the wearable control mode. The joystick however may have the advantage in another way. A study by Langolf et al. (1976), determined that small movements with fingers yield higher throughput than larger arm movements at the shoulder. Our wearable system relies solely on large movements at the elbow and shoulder joints. Balakrishnan and MacKenzie (1997) studied the movement of the finger, wrist, and forearm, but not the entire arm. In contrast to Langolf et al., they observed a higher throughput for the wrist and forearm than the index finger.

5.2 Latency Issues

It became apparent over the course of both studies that latency issues were significantly affecting system performance. In the first experiment the lag was visually noticeable. A study measuring human neural response through magnetoencephalography determined that the time between the perception of visual stimulus to manual reaction was on the order of 150 to 200 ms (Amano et al., 2006). Another study observed a response time to visual stimuli on the order of 180 to 200 ms (Thompson et al, 1992). MacKenzie and Ware (1993) observed that at lag of 225 ms movement times and error rates increased by 64% and 214% respectively while throughput decreased by 46.5%. Although not directly comparable, due to conformity issues with ISO 9241-9 standards, our throughputs were less than half of the throughputs observed in similar teleoperator studies. Likewise, our movement times were generally more than double the values measured by the other researchers.

Latency in the second experiment was also visually noticeable. The depth cursor on screen in the 3D fish tank virtual reality environment visibly trailed behind the user's arm movements. Again, the same penalties to throughput and movement time apply. The results of our study yielded an average throughput of rough 0.94 bits/s. A similar study using the NaturalPoint *OptiTrack* system and Fitts' 3D task generated throughputs on ranging from 1.5 to 3.0 bits/s (Teather and Stuerzlinger, 2011). Their movement times ranged from roughly 1.0 to 2.4 seconds while our results were on the order of 3.0 seconds. These penalties in movement time and throughput are consistent with the observations of the effects of latency.

5.3 Sensor Issues

Another factor in our wearable system is the placement of the sensors on users. Our approach was to attach the sensors to Velcro straps worn on the upper arm and forearm.

Bruggemann et al. (2013) mounted their sensors on a jacket worn by users, since it was important that the sensors were securely mounted on the user. As the trials progressed it was observed that if the sensors were not securely placed, they would slip thus introducing a progressive displacement error in tracking position and orientation. During the user study, the sensor system was constantly recalibrated to maintain accuracy. Ensuring that the Velcro straps were tight enough to prevent slippage and yet still be comfortable was problematic. The weight of the sensor prototypes were substantial enough to cause slippage with the constant arm movement, but a more compact and lighter design may ameliorate this design consideration.

5.4 System Design Considerations

Examining the overall system for possible sources of latency is a difficult and complicated task. Starting from the sensors, the sampling rate of each accelerometer/gyro unit was set to 25 Hz yielding one sample every 40 ms. A lag of 40 ms is significant as determined by MacKenzie and Ware (1993). Higher sampling rates are possible, up to 100 Hz, but the FIFO buffer was unstable. Communications with the sensors to the host computer were implemented through Digikey *Xbee* radios running at 57600 bps. Each packet containing quaternion data sent from the Arduino is approximately 150 bits, thus the data transfer rate is approximately 384 packets per second. Thus the bottleneck in the sensor and communication system to the host computer is the 40 ms sampling rate. Increasing the wireless data rate would be futile. Each sensor communicates on its own wireless channel with the host computer to eliminate the risk of packet collisions and resends.

The next step in the chain is the Java based Processing programming environment. The code imports the raw quaternion data from the sensors and performs calculations such as inverse kinematics in the case of Experiment 1 to send to the servo motor controller of the Lynxmotion robot arm. The software must also detect the click, dwell, and twist selection events in the case of Experiment 2. The RxTx package for Java serial communications specifies a polling interval of serial/USB ports of 20 ms. This is less than half the sampling rate of the accelerometer/gyro sensors and acceptable in the overall system. Should the sampling rate increase, the polling interval will have shorten to accommodate the increased packet rate. The Processing code does not use serial port interrupts, but polls the serial ports in an infinite loop. It is unknown whether the host computers running at 2.6 GHz and 2.9 GHz respectively for Experiments 1 and 2 is able to generate and output data fast enough to keep pace with the packets coming from each sensor at 25 Hz. The Processing code also draws a wire frame representation of the user's arm continuously in order to visually verify that calibration of each sensor is maintained throughout each block of trials. In Experiment 2, two monitors are used with the host computer. One of the monitors shows the wire frame motion, while the 3D monitor depicts the fish tank virtual reality working environment. This may be the cause of a possible system bottleneck. It is possible that the NVIDIA *GTX 560 TI* is unable to handle the demands of rendering images to both monitors simultaneously, particularly since the 3D monitor runs at a full HD resolution of 1920 × 1080 at a refresh rate of 120 Hz.

In Experiment 1, for the wearable system, the output of the Processing code consists of angles sent at a data rate of 115200 bps to our servo motor controller, an Arduino *UNO* running at 16 MHz. Joystick control of the robotic arm was implemented by communicating with Lynxmotion's *SSC-32* control software through a USB port, then onwards at a data rate of 115200 bps to the Lynxmotion servo controller running at 14.75 MHz. The servo motor controllers and data connections at 115200 bps are unlikely to be the source of latency. However, the physical properties of the robotic arm may be a significant factor. The performance of the servo motors in the system in conjunction with the mass and momentum of the arm itself could possibly contribute to lag in the system.

After the robotic arm, the next step in the chain is the test apparatus reproducing Fitts' original experiment. Target and error plates are read by another Arduino *UNO* which communicates with the host computer at 57600 bps. The test apparatus software runs on Java Eclipse, so again has the 20 ms serial port polling period. It is possible that this in conjunction with the either the Processing software or the Lynxmotion *SSC-32* software is a potential source of delay.

In Experiment 2, the Processing software outputs three dimensional position information in the form of a text file which is then read by a modified version of the fish tank VR software provided by Teather and Stuerzlinger (2013). This software generates the log data for the user study. It is possible that this software, or the transfer of data through a text file is a source of system delay.

CHAPTER 6 - CONCLUSIONS AND FUTURE WORK

Our wearable system was observed to perform just as well as the de facto joystick standard in a one-dimensional Fitts' task. There were no significant differences in movement time nor throughput. However, the error rate was almost twice as high. Throughput was slow compared to other studies with a telemanipulator, but direct comparisons may not be valid due to conformity issues with the ISO 9241-9 standard.

Performance of our system to control a depth cursor in fish tank VR was low, yielding long movement times on the order of 3 seconds, and low throughputs averaging roughly 0.94 bits per second. In comparison, Teather and Stuerzlinger achieved scores roughly twice as high as ours. The selection methods performed roughly the same in all measures except for error rates which are understandable. The dwell method defines a zero percent error rate. The error rate for the twist method was half that of the click method at roughly 3.5% vs. 7.0%. Again this was probably due to the implementation of a "sticky" function with the twist method to compensate for the Heisenberg Effect. Overall there were no clear differences in comfort, ease of use, or preference in either of the three methods even with the de facto standard button click method.

Future work to improve the system performance would require finding and mitigating sources of lag. As noted by others, one cannot simply insert timestamps within the system to attempt to measure latency internally. Teather et al. (2009) measured the latency of a baseline mouse-based system and the NaturalPoint *OptiTrack* camera based system with an arrangement including a pendulum and a digital video camera This system would be suitable for both Experiments 1 and 2. The latency of the NaturalPoint system was observed to be on the order of 70 ms. Our system had visible lag in both the telemanipulator performance and in fish tank VR. This indicates that there is at least a 150 to 200 ms lag according to neurological studies. Until this problem is addressed, our system will suffer a performance penalty.

REFERENCES

Amano, K., Goda, N., Nishida, S., Ejima, Y., Takeda, T., Ohtani, Y., Estimation of the timing of human visual perception from magnetoencephalography. *The Journal of Neuroscience*, 26 (15), 2006, 3981–3991

Argelaguet, F. and Andujar, C., A survey of 3D object selection techniques for virtual environments. *Computers & Graphics*, 2013, *37(3)*, 121-136.

Balakrishnan, R. and MacKenzie, I. S., Performance differences in the fingers, wrist, and forearm in computer input control, In *Proceedings of the CHT '97 Conference on Human Factors in Computing Systems*, (New York: ACM, 1997), 303–310.

Biggs, S. J. and Srinivasan, M. A., Haptic interfaces. *Handbook of Virtual Environments: Design, Implementation, and Applications*, (K. S. Hale and K. M. Stanney, Eds). Boca Raton, FL: CRC Press, Taylor & Francis Group, 2002, 93–116.

Bowman, D. A., Johnson, D. B., & Hodges, L. Fl., Testbed evaluation of virtual environment interaction techniques. In *VRST '99: Proceedings of the ACM symposium on Virtual reality software and technology*, (New York: ACM, 1999), 26–33.

Bowman, D. A., Wingrave, C. A., Campbell, J. M., Ly, V. Q., & Rhoton, C. J., Novel uses of pinch gloves for virtual environment interaction techniques, *Virtual Reality*, 6, 2002, 122 - 129.

Bruggemann, B., Gaspers, B., Ciossek, A., Pellenz, J., & Kroll, N., Comparison of different control methods for mobile manipulation using standardized tests. *IEEE International Symposium on Safety, Security, and Rescue Robotics* - *SSRR 2013*, (New York: IEEE, 2013), 1–2.

Card, S. K., English, W. K., & Burr, B. J., Evaluation of mouse, rate-controlled isometric joystick, step keys, and text keys for text selection on a CRT. *Ergonomics, 21*, 1978, 601–613.

Cha, Y. and Myung, R., Extended Fitts' law for 3D pointing tasks using 3D target arrangements. *International Journal of Industrial Ergonomics*, 2013, *43(4)*, 350-355.

Chen, J. Y., Haas, E. C., & Barnes, M. J., Human performance issues and user interface design for teleoperated robots. *Systems, Man, and Cybernetics, Part C: Applications and Reviews, IEEE Transactions on, 37(6)*, (New York: IEEE, 2007) , 1231-1245.

Chien, J. H., Tiwari, M. M., Suh, I. H., Mukherjee, M., Park, S. H., Oleynikov, D., & Siu, K. C., Accuracy and speed trade-off in robot-assisted surgery. *The International Journal of Medical Robotics and Computer Assisted Surgery*, *6(3)*, 2010, 324–329.

Cockburn, A., Quinn, P., Gutwin, C., Ramos, G., & Looser, J., Air pointing: Design and evaluation of spatial target acquisition with and without visual feedback. *International Journal of Human-Computer Studies*, 2011, *69(6)*, 401-414.

Crampton, N., Fox, K., Johnston, H., & Whitehead, A., Dance, dance evolution: Accelerometer sensor networks as input to video games. In *Haptic, Audio and Visual Environments and Games, 2007. HAVE 2007. IEEE International Workshop on*, (New York: IEEE, 2007), 107-112.

Deber, J., Araujo, B., Jota, R., Forlines, C., Leigh, D., Sanders, S., & Wigdor, D., Hammer Time!: A Low-Cost, High Precision, High Accuracy Tool to Measure the Latency of Touchscreen Devices. In *Proceedings of the 2016 CHI Conference on Human Factors in Computing Systems,* (New York: ACM, 2016), 2857-2868.

Douglas, S. A., Kirkpatrick, A. E., & MacKenzie, I. S., Testing pointing device performance and user assessment with the ISO 9241, Part 9 standard. In *Proceedings of the SIGCHI Conference on Human Factors in Computing Systems - CHI 1999*, (New York: ACM, 1999), 215–222.

Draper, J. V. and Handel, S., End-effector velocity and input frequency effects on teleoperator performance. In *Proceedings of the Human Factors and Ergonomics Society Annual Meeting*. Thousand Oaks, CA: SAGE Publications, 1989, *33(10)*, 584-588.

Draper, J. V., Handel, S., & Hood, C. C., Fitts' Task by teleoperator: Movement time, velocity, and acceleration. In *Proceedings of the Human Factors and Ergonomics Society Annual Meeting.* Thousand Oaks, CA: SAGE Publications, 1990, *34(1)*, 127-131.

Ellis, R. D., Cao, A., Pandya, A., Composto, A., Chacko, M., Klein, M., & Auner, G., Optimizing the surgeon-robot interface: The effect of control-display gain and zoom level on movement time. *Proceedings of the Human Factors and Ergonomics Society Annual Meeting - HFES 2004.* Thousand Oaks, CA: Sage Publications, 2004, *48(15)*, 1713–1717.

Epps, B. W., Comparison of six cursor control devices based on Fitts' law models. In *Proceedings of the 30th Annual Meeting of the Human Factors Society*. Santa Monica, CA: Human Factors Society, 1986, 327-331.

Farella, E., Benini, L., Ricco, B., & Acquaviva, A., Moca: A low-power, low-cost motion capture system based on integrated accelerometers. *Advances in Multimedia*, *2007, 1*, 1.

Fitts, P. M., The information capacity of the human motor system in controlling the amplitude of movement. *Journal of Experimental Psychology*, 1953, *47(6)*, 381–391.

Gallo, L., De Pietro, G., & Marra, I., 3D interaction with volumetric medical data: experiencing the Wiimote. In *Proceedings of the 1st international conference on Ambient* *media and systems*. (Belgium: ICST Institute for Computer Sciences, Social-Informatics and Telecommunications Engineering), 2008, 14.

Goertz, R., Some work on manipulator systems at ANL, past, present, and a look at the future. In *Proceedings of the 1964 Seminars on Remotely Operated Special Equipment.* Germantown, Maryland, 1964, *1*, 27-69.

Gonzalez, D., Carnahan, H., Praamsma, M., & Dubrowski, A., Control of laparoscopic instrument motion in an inanimate bench model: Implications for the training and the evaluation of technical skills, *Applied ergonomics*, 2007, *38(2)*, 123-132.

Grossman, T. and Balakrishnan, R., The design and evaluation of selection techniques for 3D volumetric displays. In *Proceedings of the 19th annual ACM symposium on User interface software and technology*, (New York: ACM, 2006), 3-12.

Hand, C., A survey of 3D interaction techniques. In *Computer graphics forum*, 1997, *16(5)*, 269-281

Hoffman, D. M., Girshick, A. R., Akeley, K., and Banks, M. S., Vergence accommodation conflicts hinder visual performance and cause visual fatigue. In *Journal of Vision*, 2008, *8 (3)*, 1-30

ISO (2000). Ergonomic requirements for office work with visual display terminals (VDTs) — Part 9: Requirements for non-keyboard input devices (ISO 9241-9). International Organization for Standardization.

Jagacinski, R. J. and Monk, D. L., Fitts' Law in two dimensions with hand and head movements. *Journal of Motor Behavior*, 1985, *17(1)*, 77–95.

Jankowski, J., and Hachet, M., A survey of interaction techniques for interactive 3D environments. In *Eurographics 2013-STAR*, 2013.

Kauderer, A., (2013). "Space station assembly." Retrieved Feb 2015, from http://www.nasa.gov/mission_pages/station/structure/elements/subsystems.html

Kim, W. S., Tendick, F., Ellis, S. R., & Stark, L. W., A comparison of position and rate control for telemanipulations with consideration of manipulator system dynamics. *IEEE Journal of Robotics and Automation,* New York: IEEE, 1987, *3(5),* 426–436.

Koo, K. M., Kim, Y. J., & Seo, Y. H., Motion capture based dual arm control of a humanoid robot using kinect, In *Information Technology Convergence*, (H. L. Barolli, F. Xhafa, H.Y. Jeong, Eds.). Netherlands: Springer, 2013, 913–921.

Kopper, R., Bowman, D. A., Silva, M. G., & McMahan, R. P., A human motor behavior model for distal pointing tasks. *International journal of human-computer studies*, *68*(10), 2010, 603-615.

Langolf, G. D., Chaffin, D. B., & Foulke, J. A., An investigation of Fitts' Law using a wide range of movement amplitudes. *Journal of Motor Behavior*, 1976, *8(2)*, 113-128.

Lapointe, J. F., Robert, J. M., & Boulanger, P., Optimizing performance in heavy equipment teleoperation. In *Proceedings of Minespace 2001*, Quebec, Quebec. Retrieved Dec 11, 2015, from http://iit-iti.nrc-cnrc.gc.ca/iit-publications-iti/docs/NRC- 44886.pdf.

Liu, L., Van Liere, R., Nieuwenhuizen, C., & Martens, J. B., Comparing aimed movements in the real world and in virtual reality. In *Virtual Reality Conference, 2009. VR 2009. IEEE*, New York: IEEE, 2009, 219-222

MacKenzie, I. S., Fitts' law as a research and design tool in human-computer interaction. *Human-computer interaction*, *7(1)*, 1992, 91–139.

MacKenzie, I. S., Fitts' throughput and the remarkable case of touch-based target selection. *Proceedings of the 16th International Conference on Human-Computer Interaction – HCII 2015*, (Berlin: Springer), 238-249.

MacKenzie, I. S. and Buxton, W., Extending Fitts' law to two dimensional tasks. *Proceedings of the CHI 1992 Conference on Human Factors in Computing Systems*, (New York: ACM, 1992), 219–226.

MacKenzie, I. S., and Oniszczak, A., A comparison of three selection techniques for touchpads. *Proceedings of the ACM SIGCHI Conference on Human Factors in Computing Systems – CHI '98*, (New York: ACM, 1998), 336-343

MacKenzie, I. S., & Teather, R. J., FittsTilt: The application of Fitts' law to tilt-based interaction. *Proceedings of the Seventh Nordic Conference on Human-Computer Interaction – NordiCHI 2012*, (New York: ACM), 568-577.

MacKenzie, I.S., and Ware, C., Lag as a determinant of human performance in interactive systems. *Proceedings of the ACM Conference on Human Factors in Computing Systems - INTERCHI '93*, (New York: ACM, 1993), 488-493.

Magee, J., Felzer, T., & MacKenzie, I. S., Camera mouse + ClickerAID: Dwell vs. single-muscle click actuation in mouse-replacement interfaces. In *Proceedings of the 16th International Conference on Human-Computer Interaction - HCII 2015* (LNCS 9170), (Switzerland: Springer, 2015), 74-84

McArthur, V., Castellucci, S. J., & MacKenzie, I. S., An empirical comparison of Wiimote gun attachments for pointing tasks. In *Proceedings of the 1st ACM SIGCHI symposium on Engineering interactive computing systems*, (New York: ACM, 2009), 203-208.

McLean, G. F., Prescott, B., & Podhorodeski, R., Teleoperated system performance evaluation. *Systems, Man and Cybernetics, IEEE Transactions on*, 1994, *24(5)*, 796-804.

Mihelj, M., Kamnik, R., & Bajd, T., Assessment of teleoperator performance. *Electrotechnical Review*, 1999, *65*, 7-13.

Mukundan, R., Quaternions: From classical mechanics to computer graphics, and beyond. *Proceedings of the 7th Asian Technology conference in Mathematics*, 2002, 97-105.

Murata, A., Extending effective target width in Fitts' Law to two dimensional pointing task. In *International Journal of Human Computer Interaction*, 1999, *11*, 137–152.

Murata, A. and Iwase, H., Extending Fitts' law to a three-dimensional pointing task. *Human movement science*, 2001, *20(6)*, 791-805.

Müller-Tomfelde, C., Dwell-based pointing in applications of human computer interaction. In *Human-Computer Interaction–INTERACT 2007*. (Berlin Heidelberg: Springer, 2007), 560-573.

Music, J., Cecić, M., & Bonković, M., Testing inertial sensor performance as hands-free human-computer interface. *WSEAS Transactions on Computers*, 2009, *8(4)*, 715-724.

Natapov, D., Castellucci, S. J., and MacKenzie, I. S., ISO 9241-9 evaluation of video game controllers. *Proceedings of Graphics Interface 2009*, (Toronto: Canadian Information Processing Society, 2009), 223–230.

Nieuwenhuizen, K., Liu, L., Van Liere, R., & Martens, J. B., Insight into 3D goal-directed movements through a division into meaningful movement phases. *IEEE Computer Graphics and Applications*, 2009, 29(6)

Pfeiffer, M., and Stuerzlinger, W., 3D virtual hand pointing with EMS and vibration feedback. *Proceedings of the IEEE Symposium on 3D User Interfaces - 3DUI'15*, (New York: IEEE Press, 2015), 117–120.

Schmitt, B., Raynal, M., Dubois, E., & Croenne, D., A composite approach to evaluate two interaction techniques for a 3D pointing task, in *Proceedings of the IEEE Symposium on 3D User Interfaces - 3DUI '12*, (New York: IEEE Press, 2012), 159–160.

Soukoreff, R. W. and MacKenzie, I. S., Towards a standard for pointing device evaluation, perspectives on 27 years of Fitts' law research in HCI. *International Journal of Human-Computer Studies*, 2004, *61(6)*, 751–789.

Stuerzlinger, W., Considerations for targets in 3D pointing experiments, *Workshop on Interactive Surfaces for Interaction with Stereoscopic 3D - ISIS3D*, 2013

Teather, R. J. (2013). *Evaluating 3D pointing techniques*. Doctoral dissertation. York University: Toronto, Ontario, Canada.

Teather, R. J., Allison, R. S. and Stuerzlinger, W., Evaluating visual/motor co-location in fish tank virtual reality, in *IEEE Toronto International Conference - Human Factors and Ergonomics Symposium, IEEE*, 2009, 624-629.

Teather, R. J., & MacKenzie, I. S., Position vs. velocity control for tilt-based interaction. *Proceedings of Graphics Interface 2014*. (Toronto: Canadian Information Processing Society, 2014), 51-58.

Teather, R. J., Pavlovych, A., Stuerzlinger, W., & MacKenzie, I. S., Effects of tracking technology, latency, and spatial jitter on object movement. In *3D User Interfaces - 3DUI 2009.* (New York: IEEE, 2009), 43-50.

Teather, R. J. and Stuerzlinger, W., Visual aids in 3D point selection experiments. In *Proceedings of the 2nd ACM symposium on Spatial user interaction*, (New York: ACM, 2014), 127-136.

Teather, R. J. and Stuerzlinger, W., Target pointing in 3D user interfaces. *Proceedings of the Graphics Interface Poster Session (GI 2010), Ottawa, Ontario, Canada, May*, 2010, 20-21.

Teather, R. J. and Stuerzlinger, W., Pointing at 3D targets in a stereo head-tracked virtual environment. In *3D User Interfaces (3DUI), 2011 IEEE Symposium on,* (New York: IEEE, 2011), 87-94.

Teather, R. J. and Stuerzlinger, W., Pointing at 3d target projections with one-eyed and stereo cursors. In *Proceedings of the SIGCHI Conference on Human Factors in Computing Systems*, (New York: ACM, 2013), 159-168.

Thompson, P. D., Colebatch, J. G., Brown, P., Rothwell, J.C., Day, B.L., Obeso, J.A., Marsden, C. D., Voluntary stimulus-sensitive jerks and jumps mimicking myoclonus or pathological startle syndromes. *Mov Disord.*, 1992, 257–62.

Van Laerhoven, K., Kern, N., Gellersen, H., & Schiele, B., Towards a wearable inertial sensor network. In *Proc. of the IEE Eurowearable*. (New York: IEEE, 2003), 125–130.

Ware, C., Arthur, K., & Booth, K. S., Fish tank virtual reality. In *Proceedings of the INTERACT'93 and CHI'93 conference on Human factors in computing systems*, (New York: ACM, 1993), 37-42.

Ware, C. and Balakrishnan, R., Reaching for objects in VR displays: Lag and frame rate. In *ACM Transactions on Computer-Human Interaction*, 1994, *1(4)*, 331–356.

Wingrave, C., Williamson, B., Varcholik, P. D., Rose, J., Miller, A., Charbonneau, E., Bott, J., & LaViola Jr, J. J., The wiimote and beyond: Spatially convenient devices for 3d user interfaces. *Computer Graphics and Applications, IEEE*, 2010, 30(2), 71-85.

Wright, E., Connolly, P. E., Sackley, M., McCollom, J., Malek, S., & Fan, K., A comparative analysis of Fish Tank Virtual Reality to stereoscopic 3D imagery. In *67th Midyear Meeting Proceedings*, 2012, 37-45.